Supplementary Information (SI) for RSC Advances.
This journal is © The Royal Society of Chemistry 2026

Chemical Reactivity of 2-Methylchromone with some Nitrogen-Based Nucleophiles: Reactions, DFT Analysis, Anticancer Activity and Molecular Docking Studies

Mohamed Abdel-Megid,[1] Najla A. Alshaye,[2] Al-Shimaa Badran[*3] and Magdy A. Ibrahim[3]

[1] *Department of Chemistry, College of Science, Imam Mohammad Ibn Saud Islamic University (IMSIU), Riyadh, Saudi Arabia.* moabmohamed@imamu.edu.sa

[2] *Department of Chemistry, College of Science, Princess Nourah bint Abdulrahman University, P.O. Box 84428, Riyadh 11671, Saudi Arabia*. naalshaye@pnu.edu.sa

[3] *Department of Chemistry, Faculty of Education, Ain Shams University, Roxy, 11711, Cairo, Egypt*

***** *E-mail*: badran.shimaa@yahoo.com,

Tel.: +2 01011444940 fax:+2 022581243

Compound	9	10
Optimized Structures	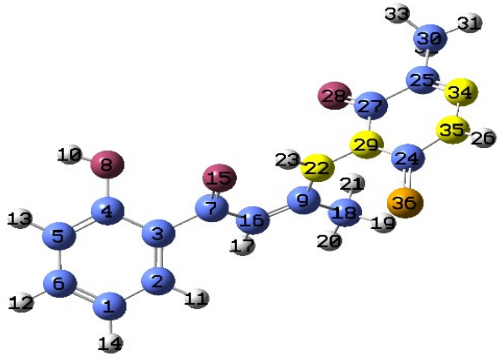	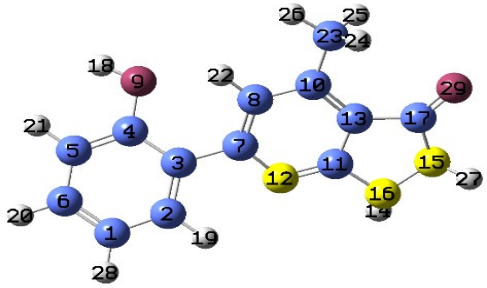
LUMO	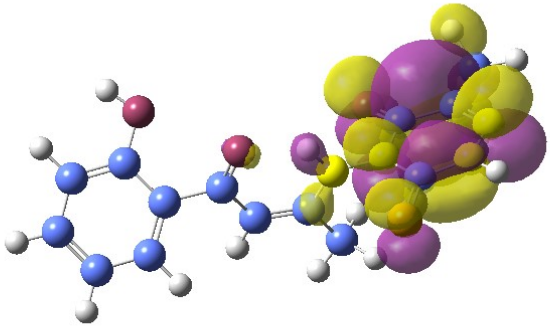 E_{LUMO} = -2.407	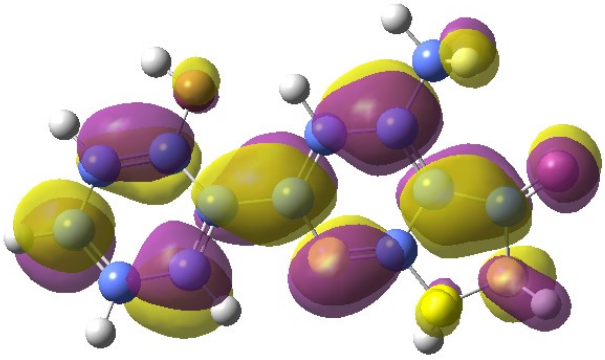 E_{LUMO} = -1.808
HOMO	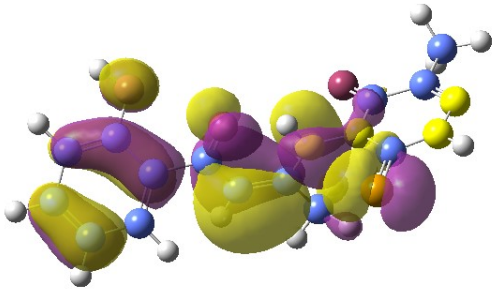 E_{HOMO}= -6.072	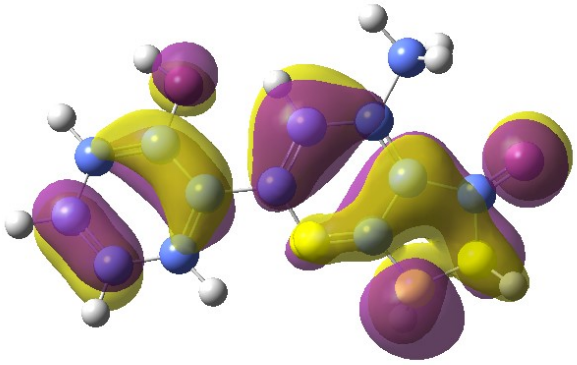 E_{HOMO}= -6.125

Fig. S1. Molecular modeling and the electron density of HOMO and LUMO of compounds **9** and **10**

Compound 12	Compound 13	Compound 14
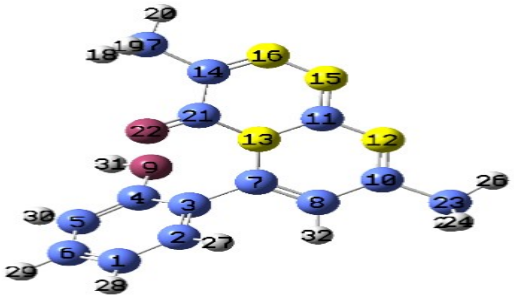	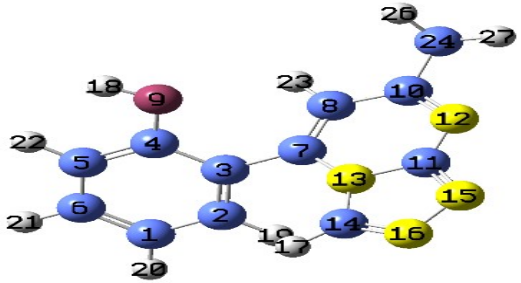	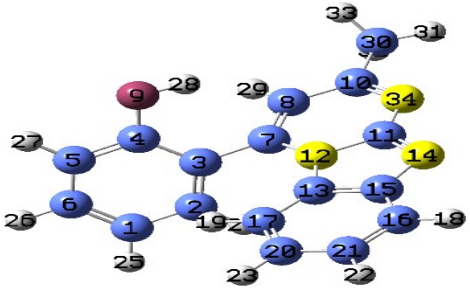
Optimized Structures	**Optimized Structures**	**Optimized Structures**
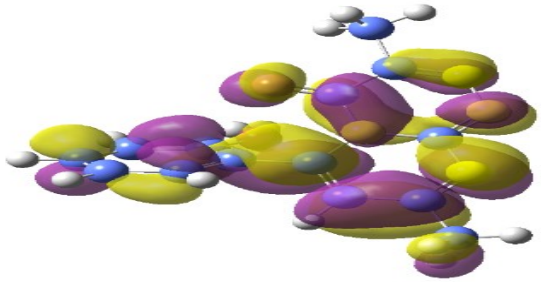	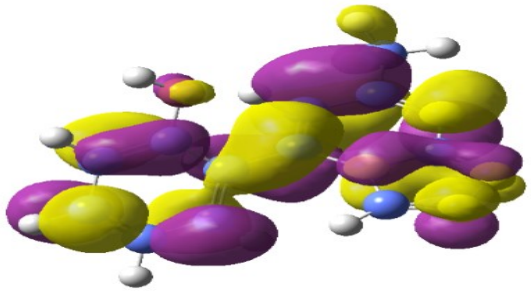	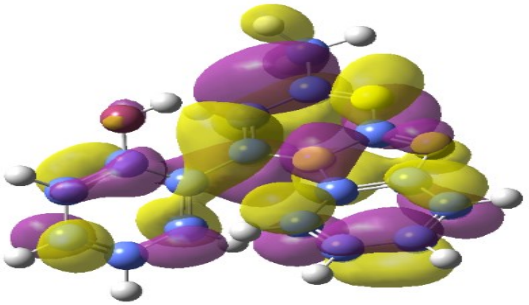
E_{LUMO} = -2.295	**E_{LUMO} = -2.046**	**E_{LUMO} = -2.074**
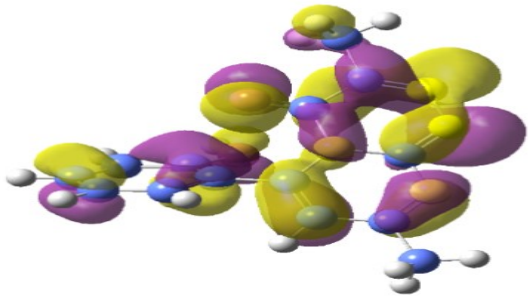	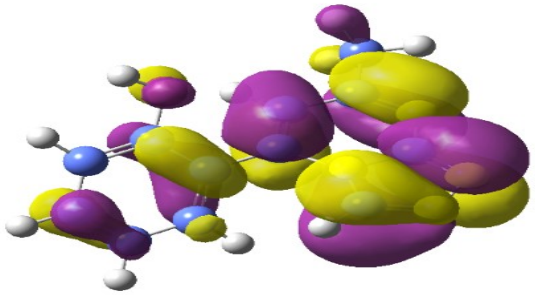	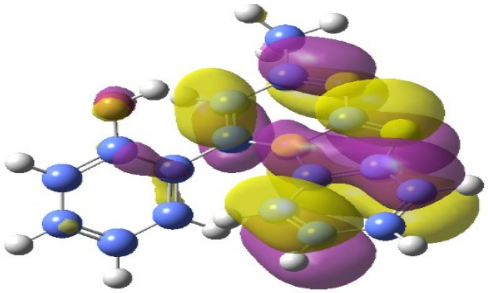
E_{HOMO}= -6.236	**E_{HOMO}= -6.350**	**E_{HOMO}= -5.965**

Fig. S2. Molecular modeling and the electron density of HOMO and LUMO of compounds **12-14**

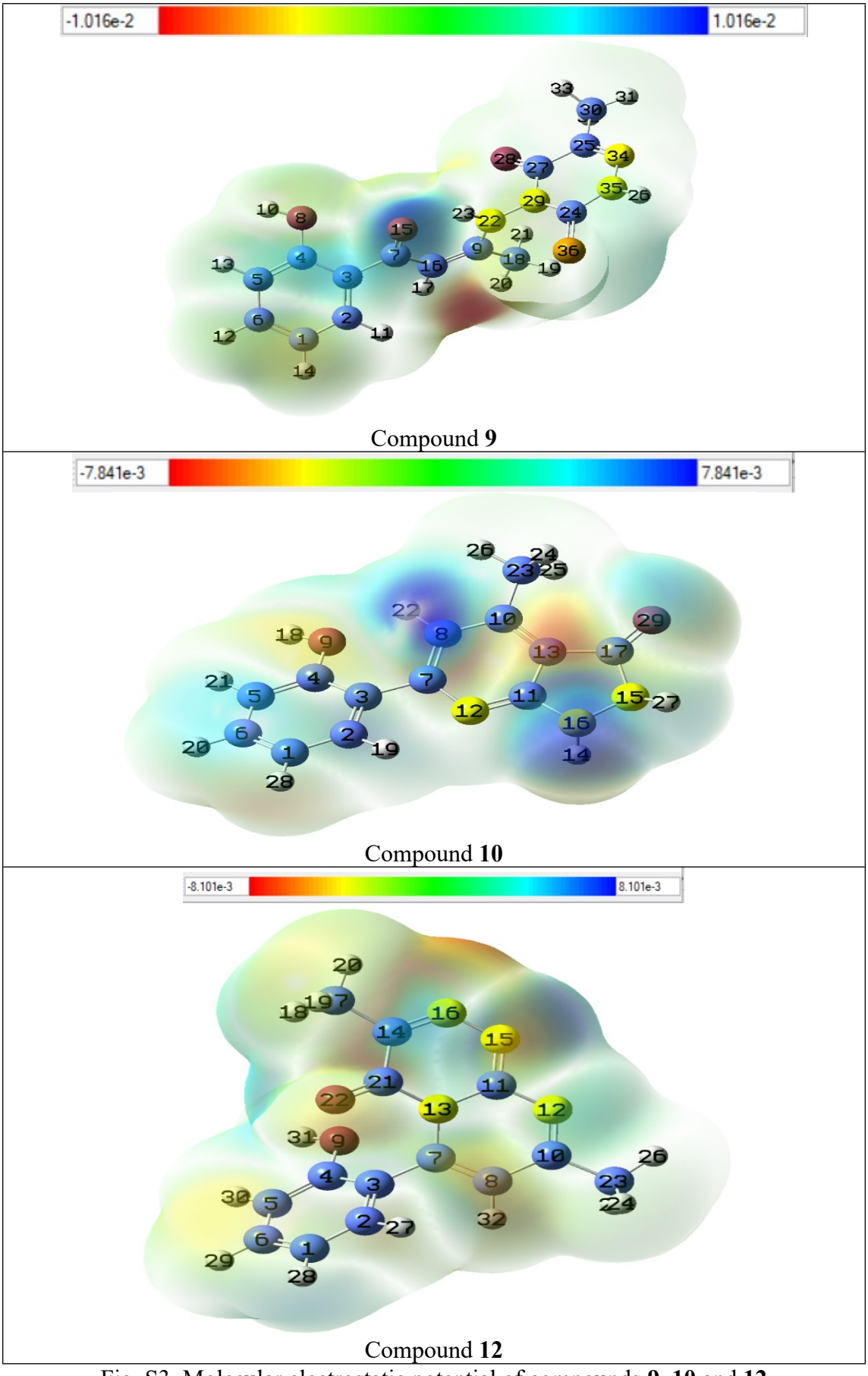

Fig. S3. Molecular electrostatic potential of compounds **9**, **10** and **12**

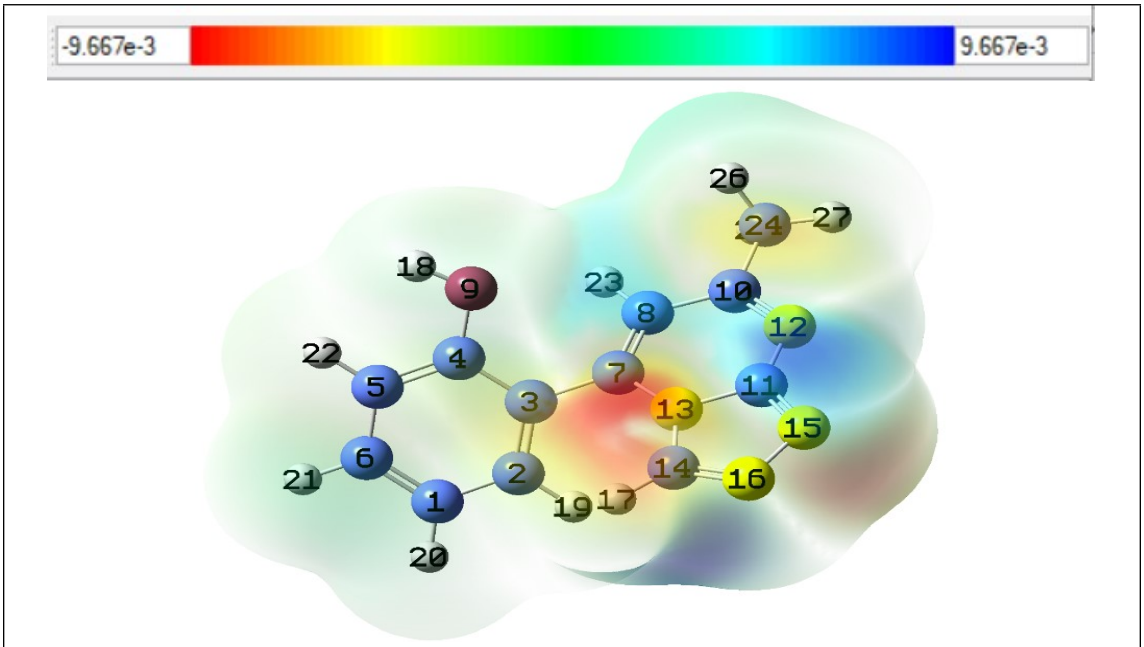

Compound **13**

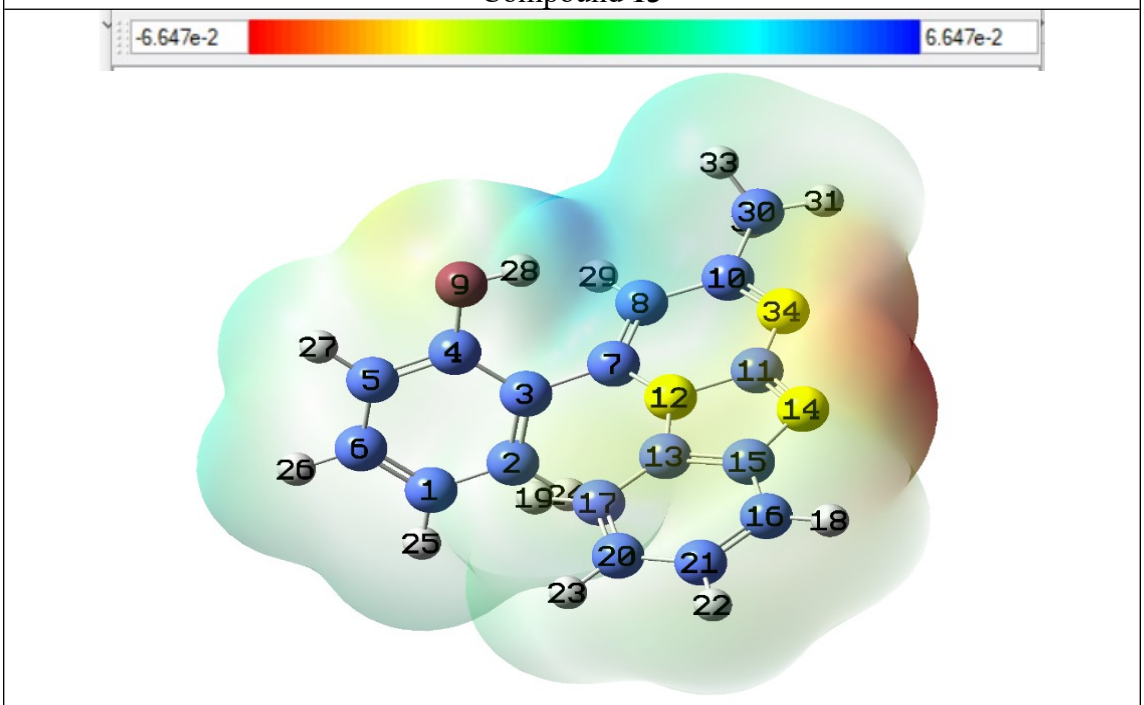

Compound **14**

Fig. S4. Molecular electrostatic potential of compounds **13** and **14**

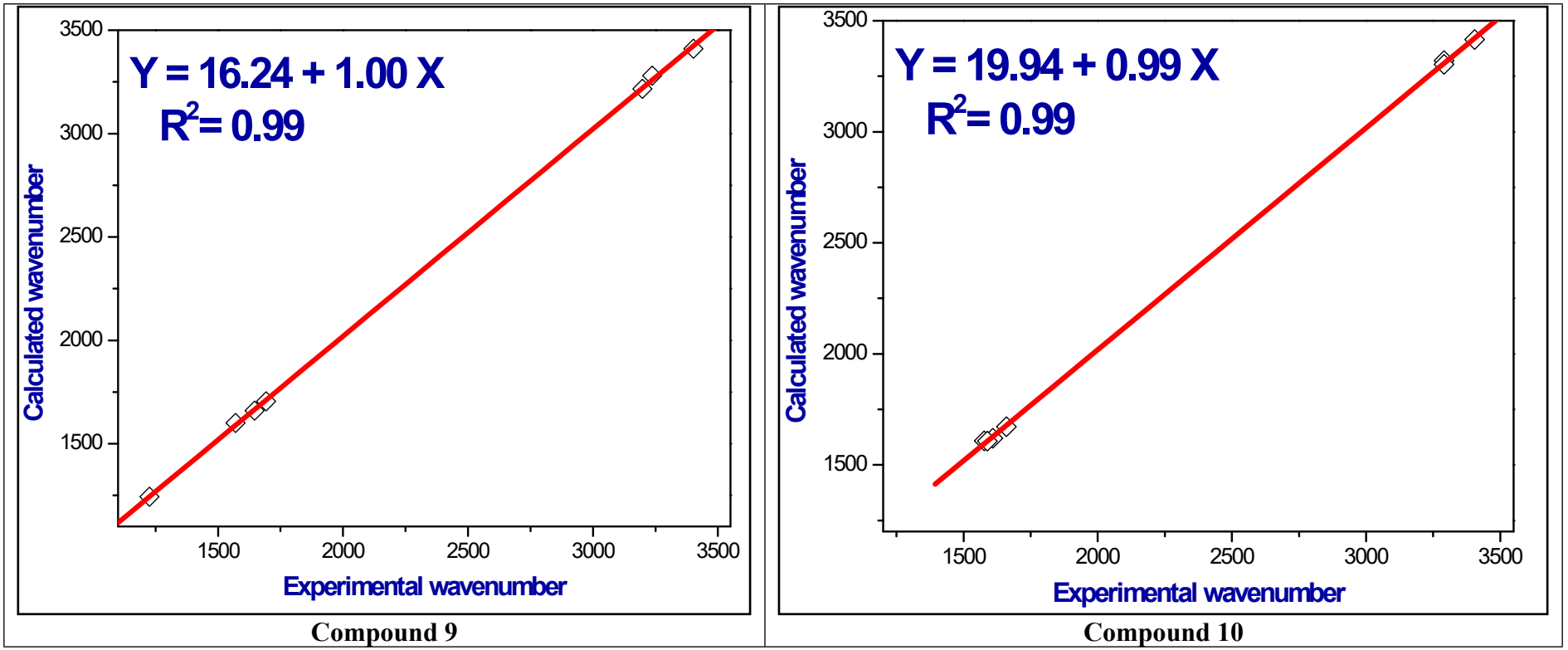

Fig. S5. The correlation relationships of the experimental *versus* calculated IR wavenumbers of compounds **9** and **10**.

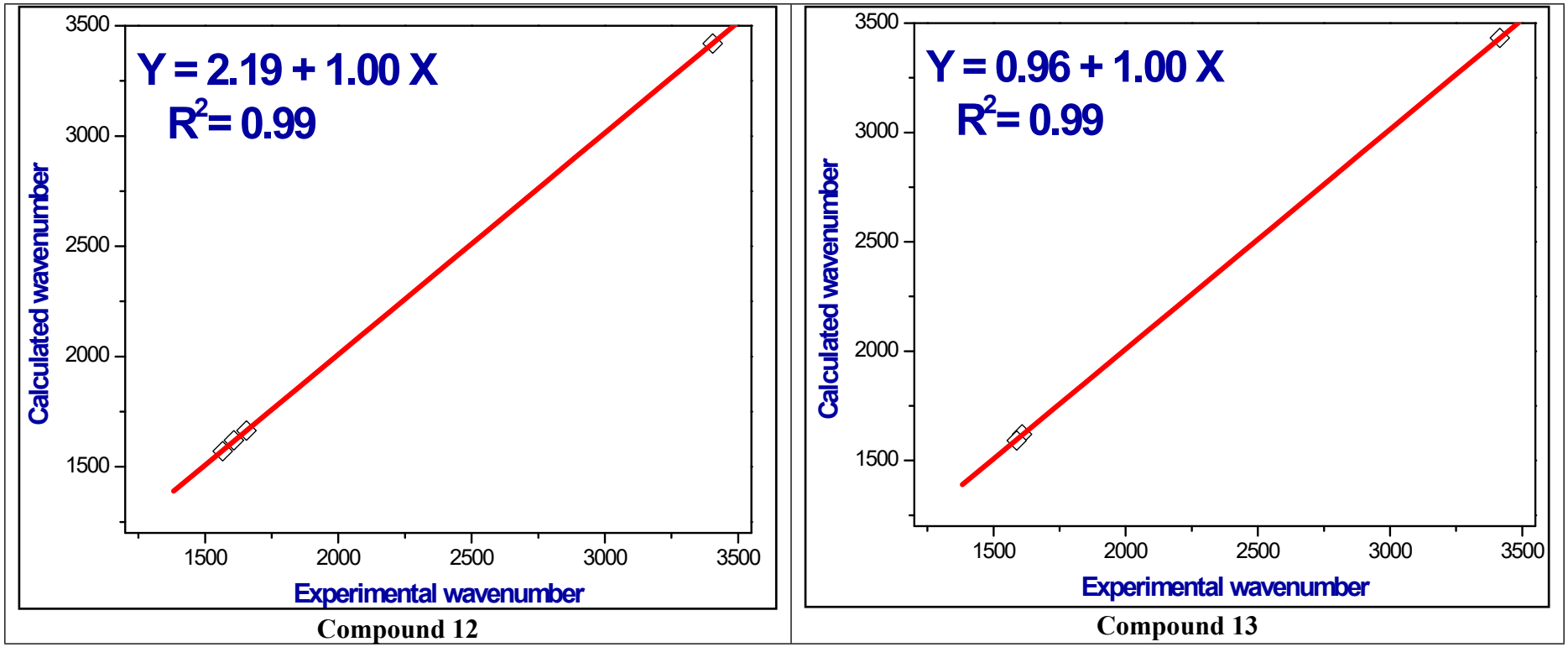

Fig. S6. The correlation relationships of the experimental *versus* calculated IR wavenumbers of compounds **12** and **13**.

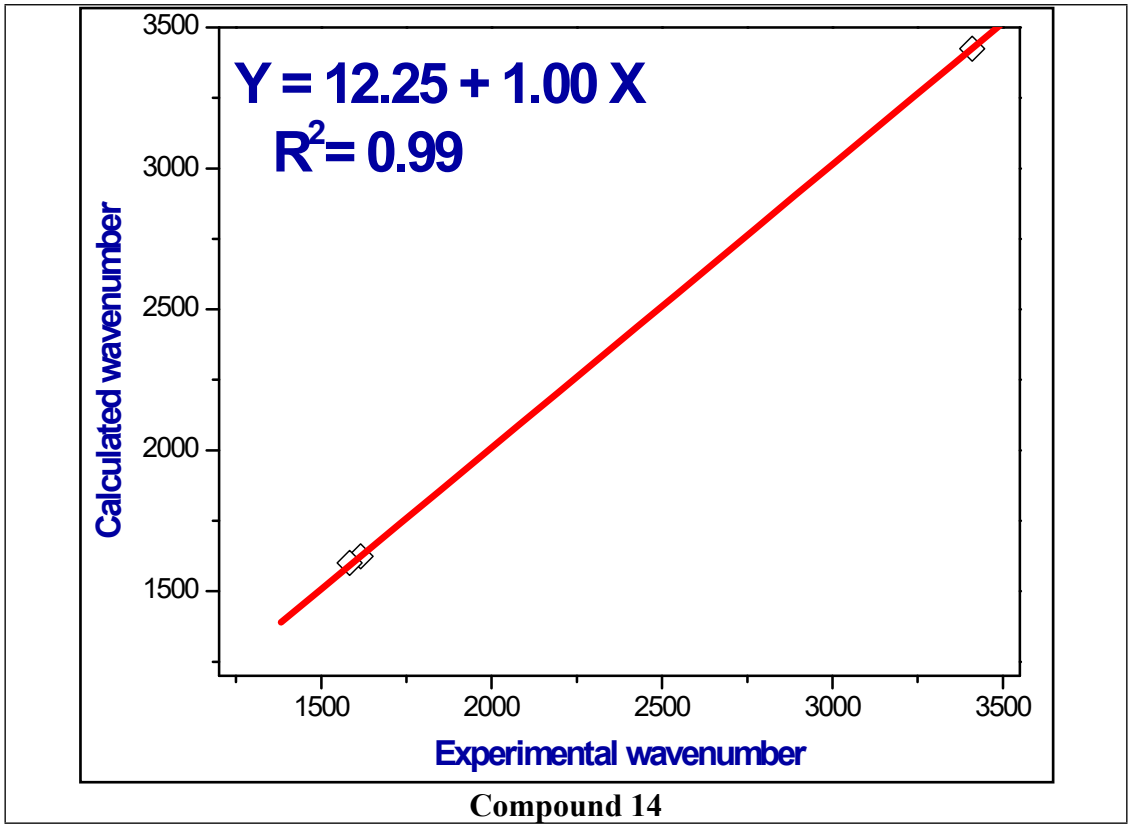

Fig. S7. The correlation relationships of the experimental *versus* calculated IR wavenumbers of compound **14**.

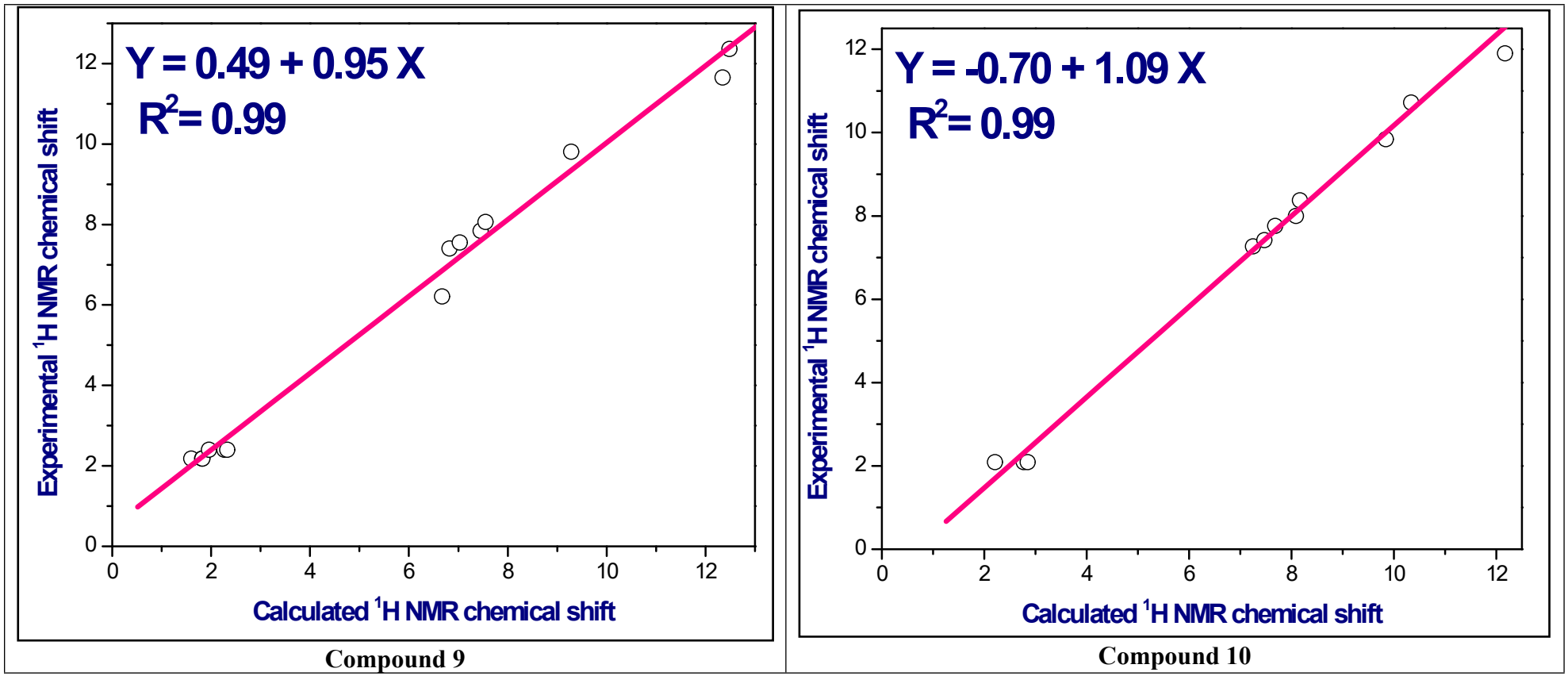

Fig. S8. The correlation relationships of the calculated *versus* experimental ^{1}H NMR chemical shifts of compounds **9** and **10**.

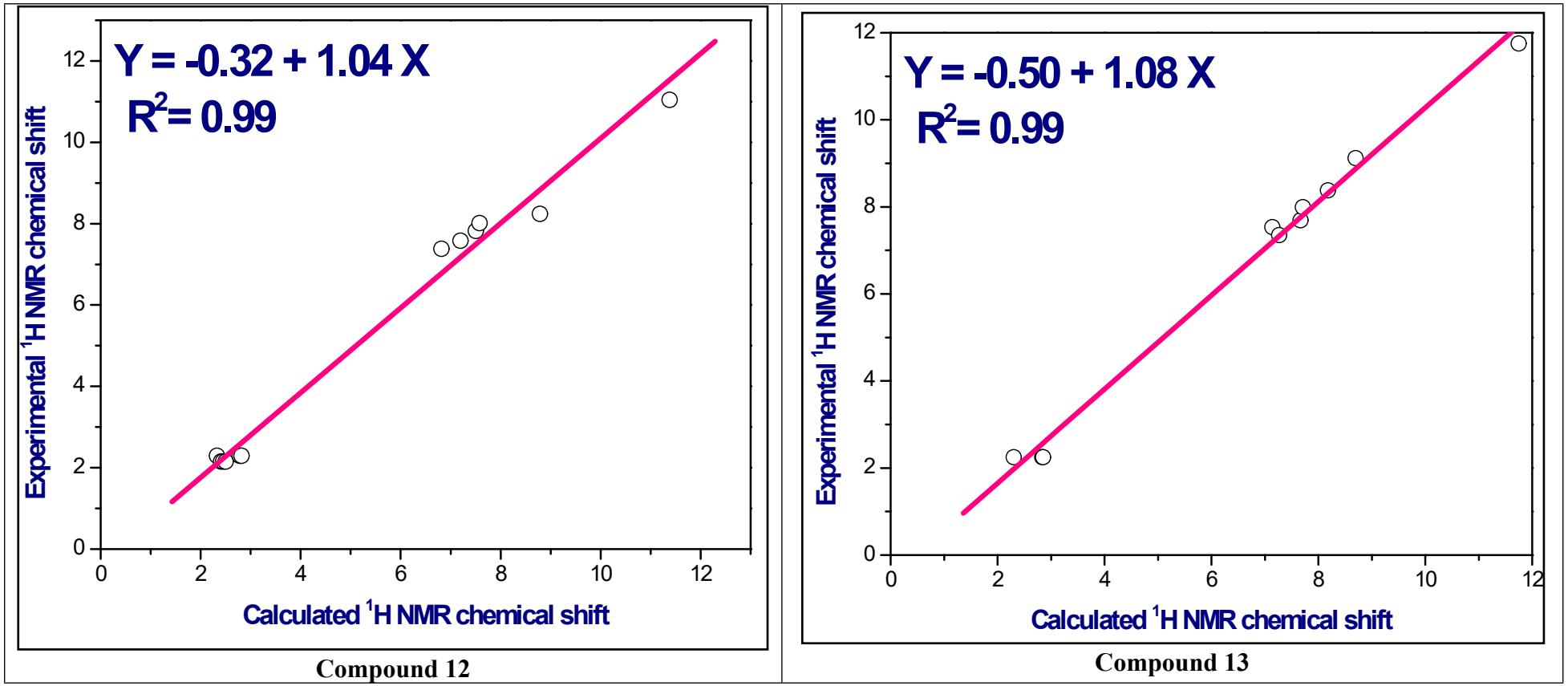

Fig. S9. The correlation relationships of the calculated *versus* experimental ^{1}H NMR chemical shifts of compounds **12** and **13**.

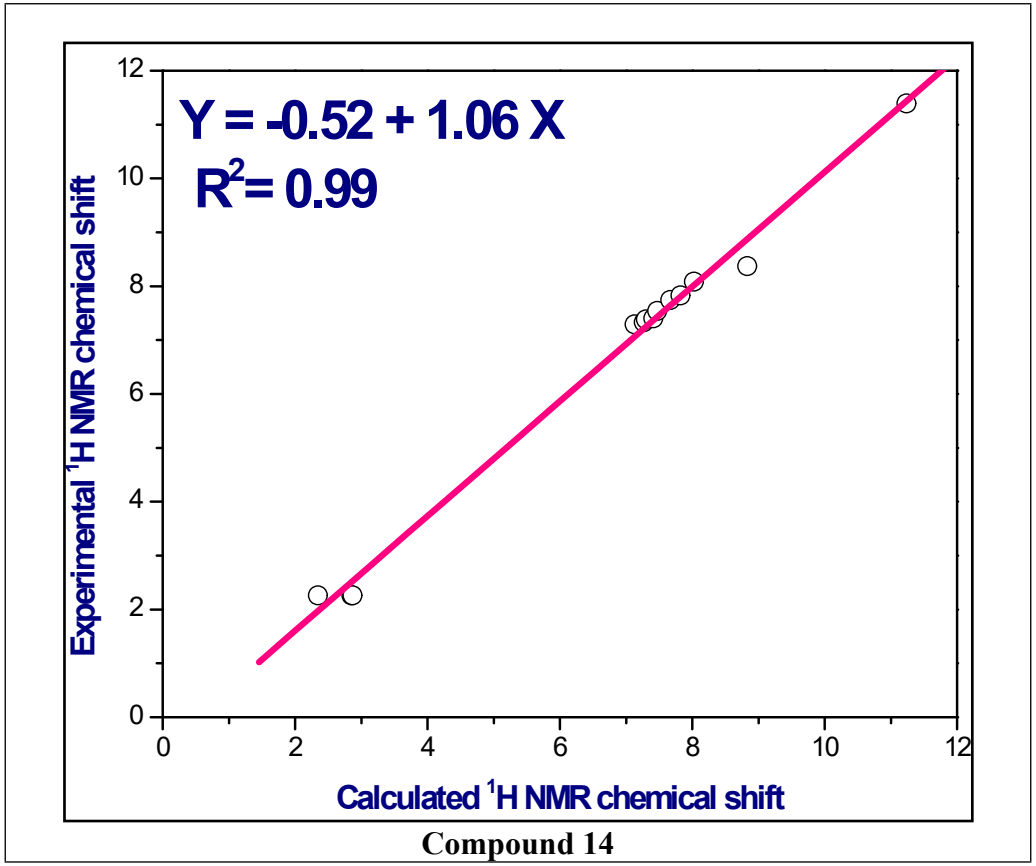

Fig. S10. The correlation relationships of the calculated *versus* experimental ^{1}H NMR chemical shifts of compound **14**.

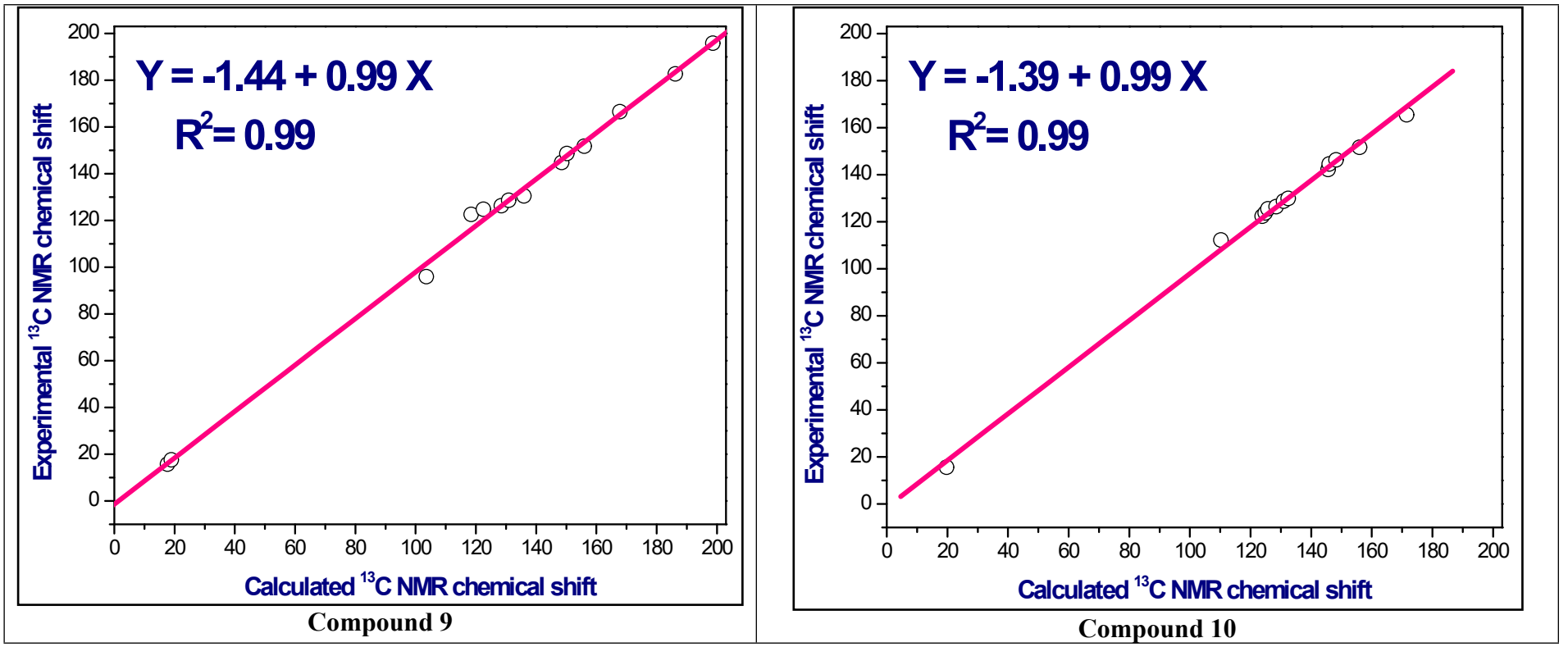

Fig. S11. The correlation relationships of the calculated *versus* experimental ^{13}C NMR chemical shifts of compounds **9** and **10**.

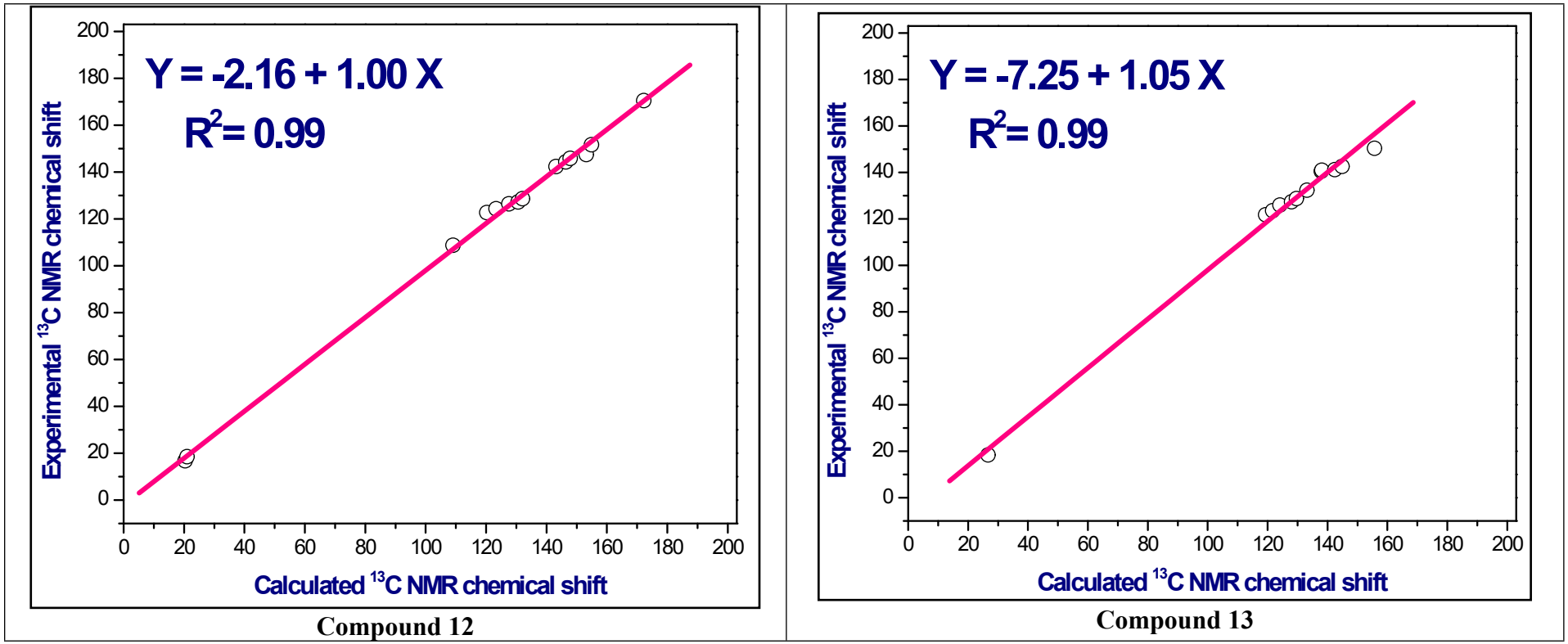

Fig. S12. The correlation relationships of the calculated *versus* experimental ^{13}C NMR chemical shifts of compounds **12** and **13**.

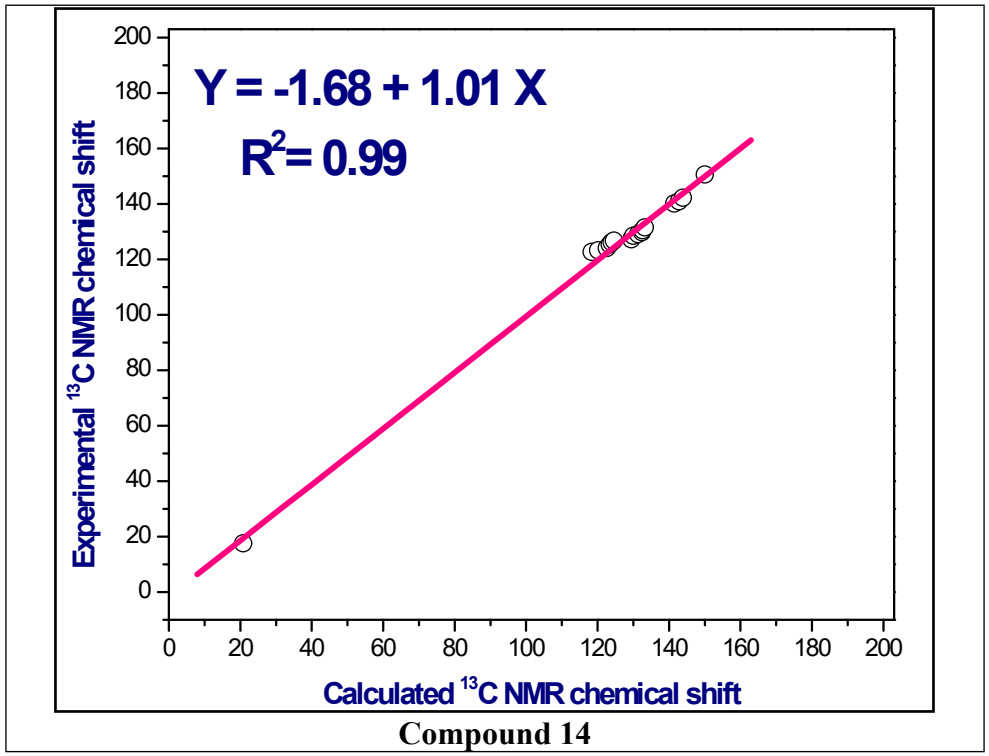

Fig. S13. The correlation relationships of the calculated *versus* experimental ^{13}C NMR chemical shifts of compound **14**.

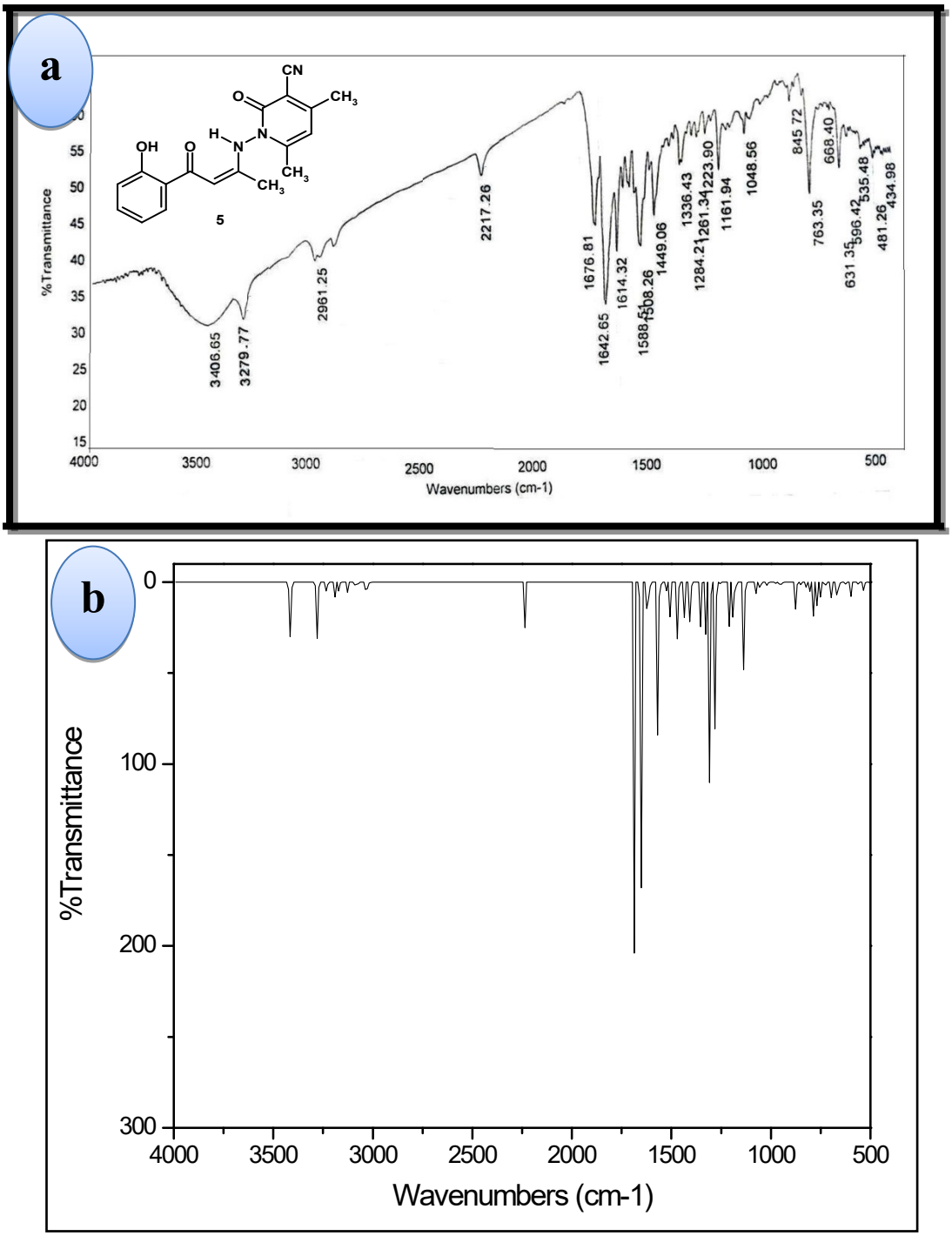

Fig. S14. (a) Experimental and (b) Calculated IR spectra of compound **5** at B3LYP/6-311++G(d,p).

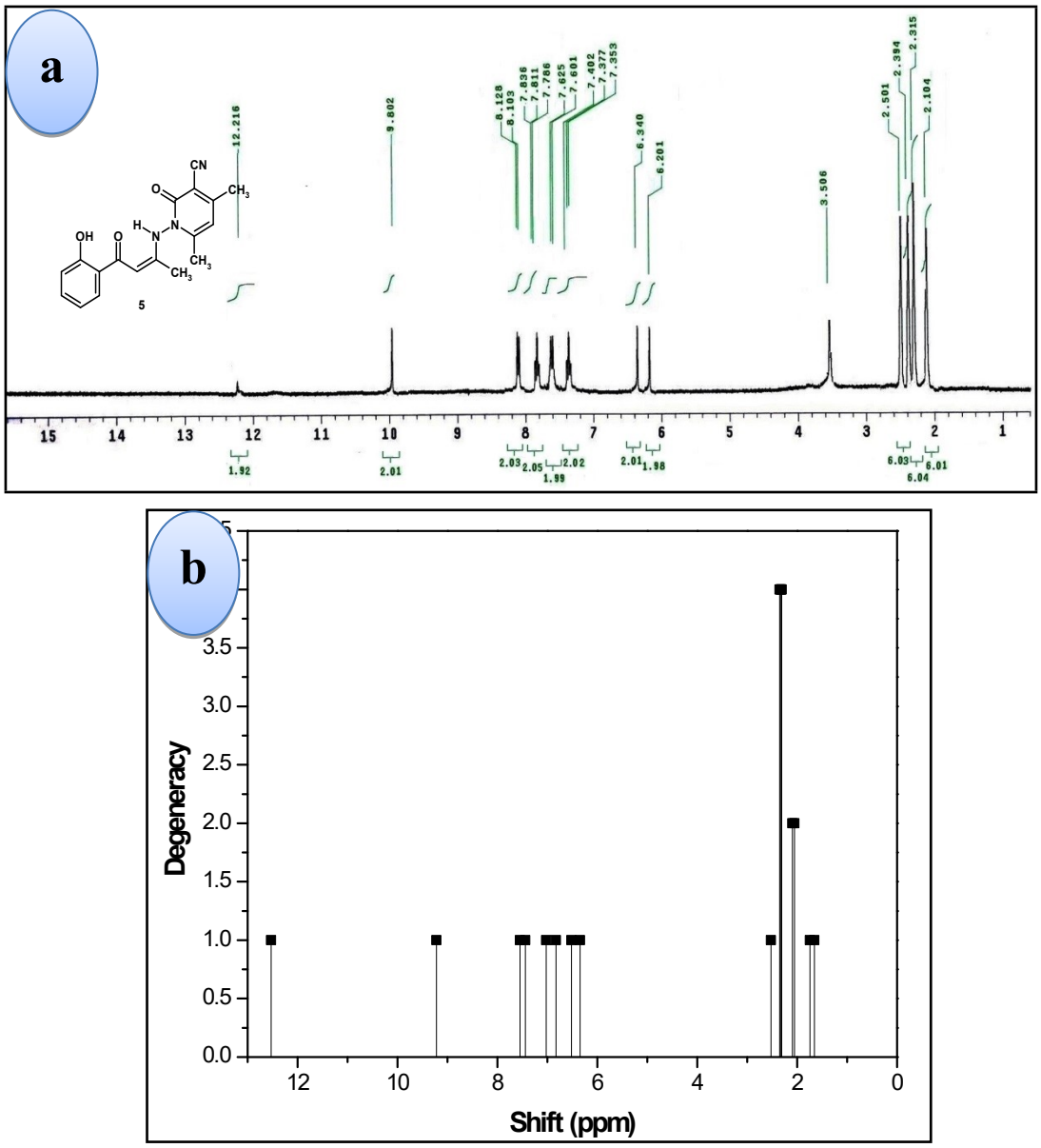

Fig. S15. (a) Experimental and (b) Calculated ^{1}H NMR spectra of compound **5** at B3LYP/6-311++G(d,p).

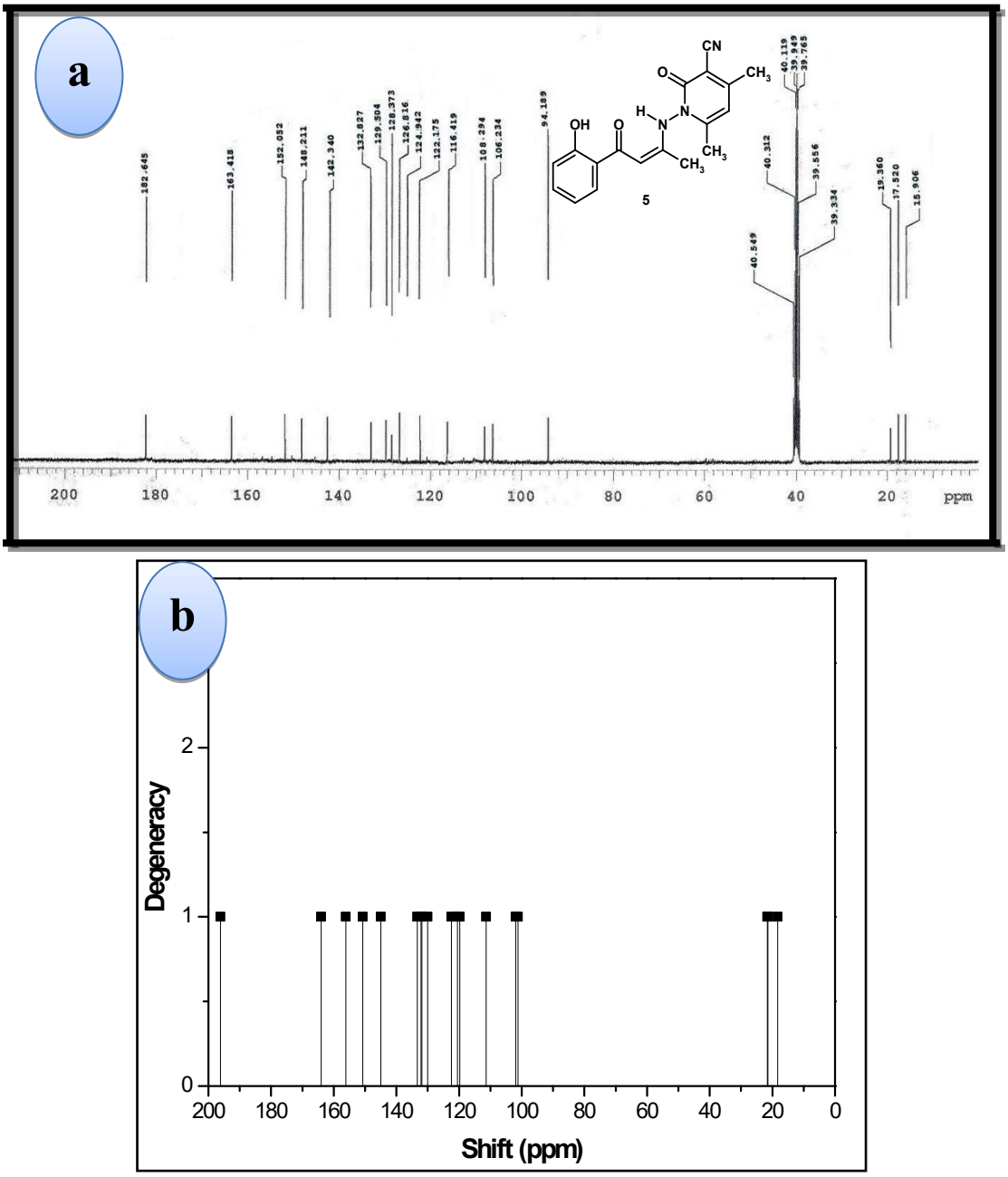

Fig. S16. (a) Experimental and (b) Calculated ^{13}C NMR spectra of compound **5** at B3LYP/6-311++G(d,p).

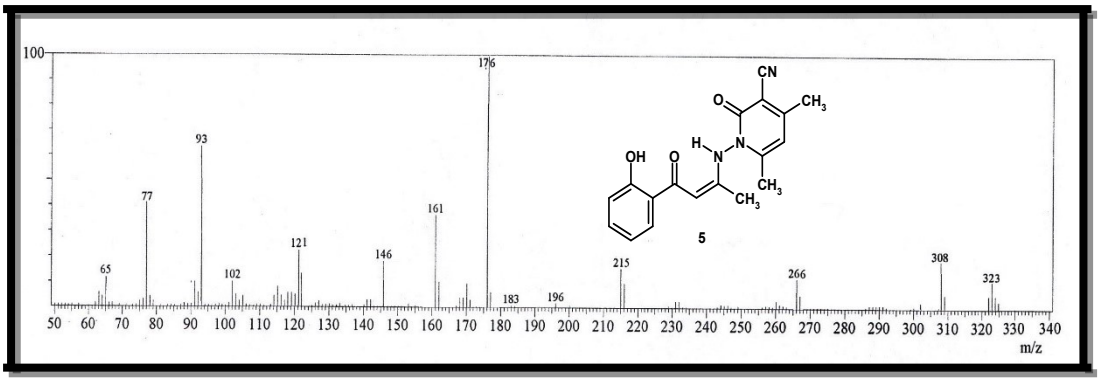

Fig. S17. Mass spectrum of compound **5**

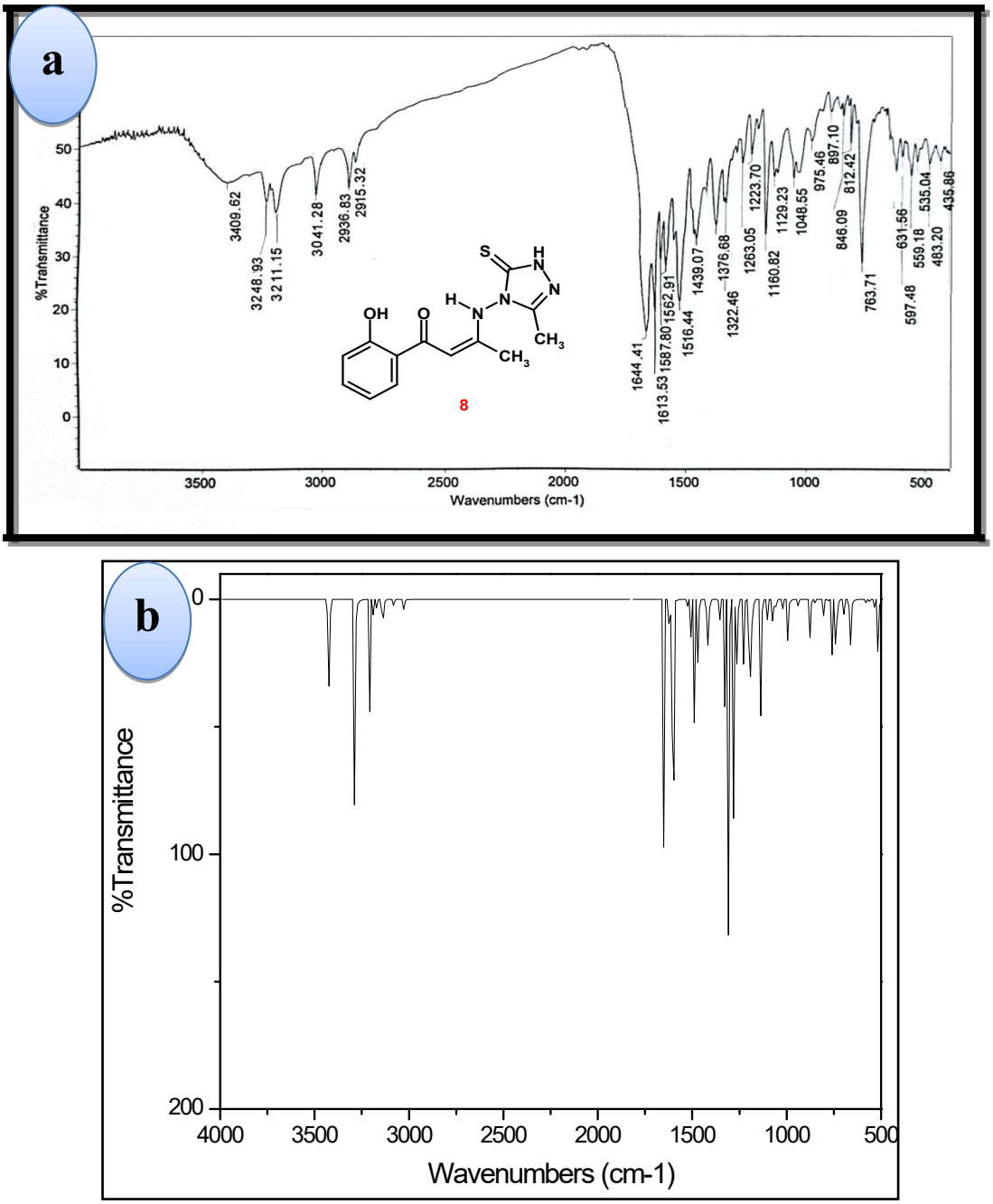

Fig. S18. (a) Experimental and (b) Calculated IR spectra of compound **8** at B3LYP/6-311++G(d,p).

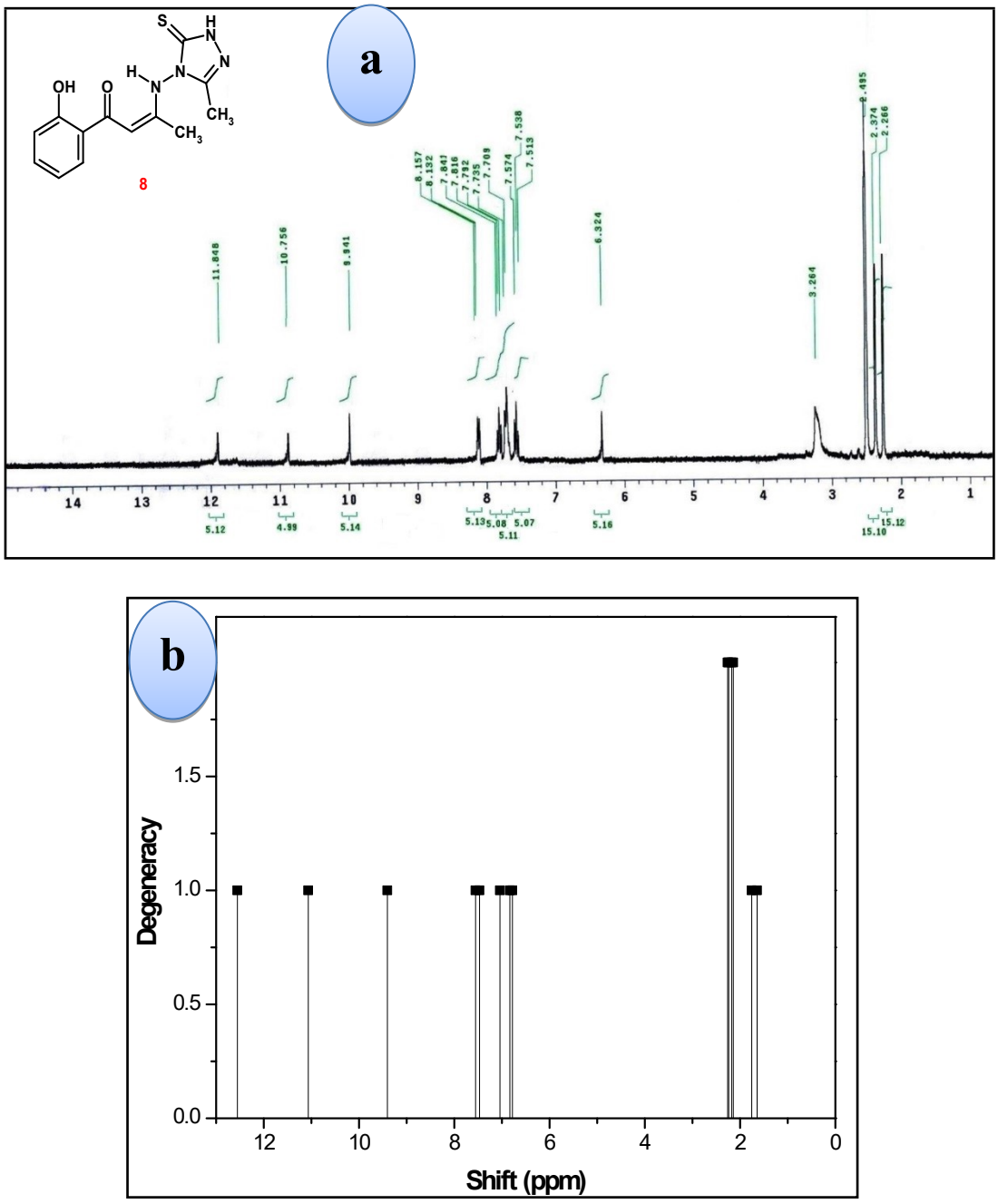

Fig. S19. (a) Experimental and (b) Calculated ^{1}H NMR spectra of compound **8** at B3LYP/6-311++G(d,p).

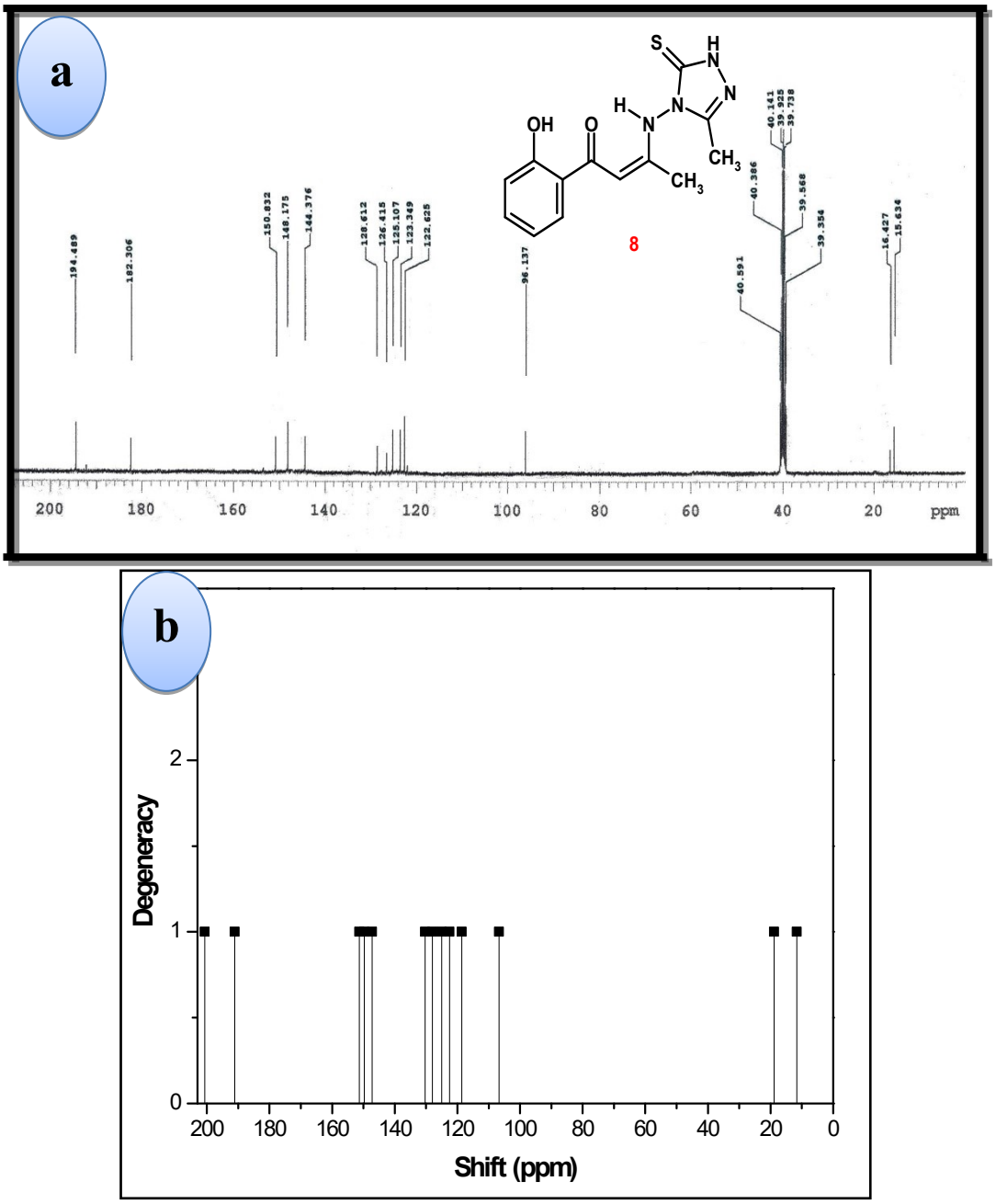

Fig. S20. (a) Experimental and (b) Calculated ^{13}C NMR spectra of compound **8** at B3LYP/6-311++G(d,p).

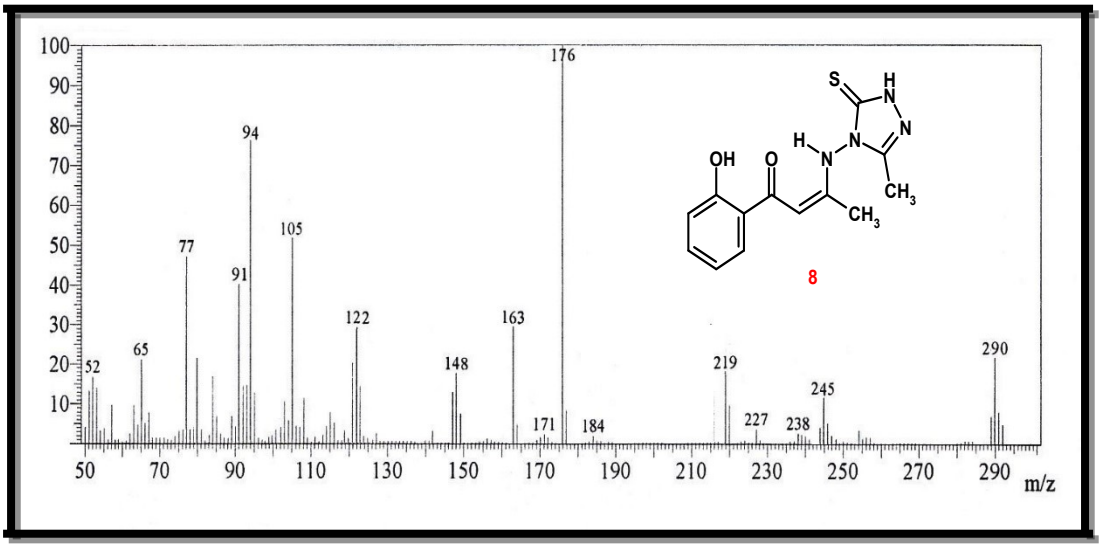

Fig. S21. Mass spectrum of compound **8**

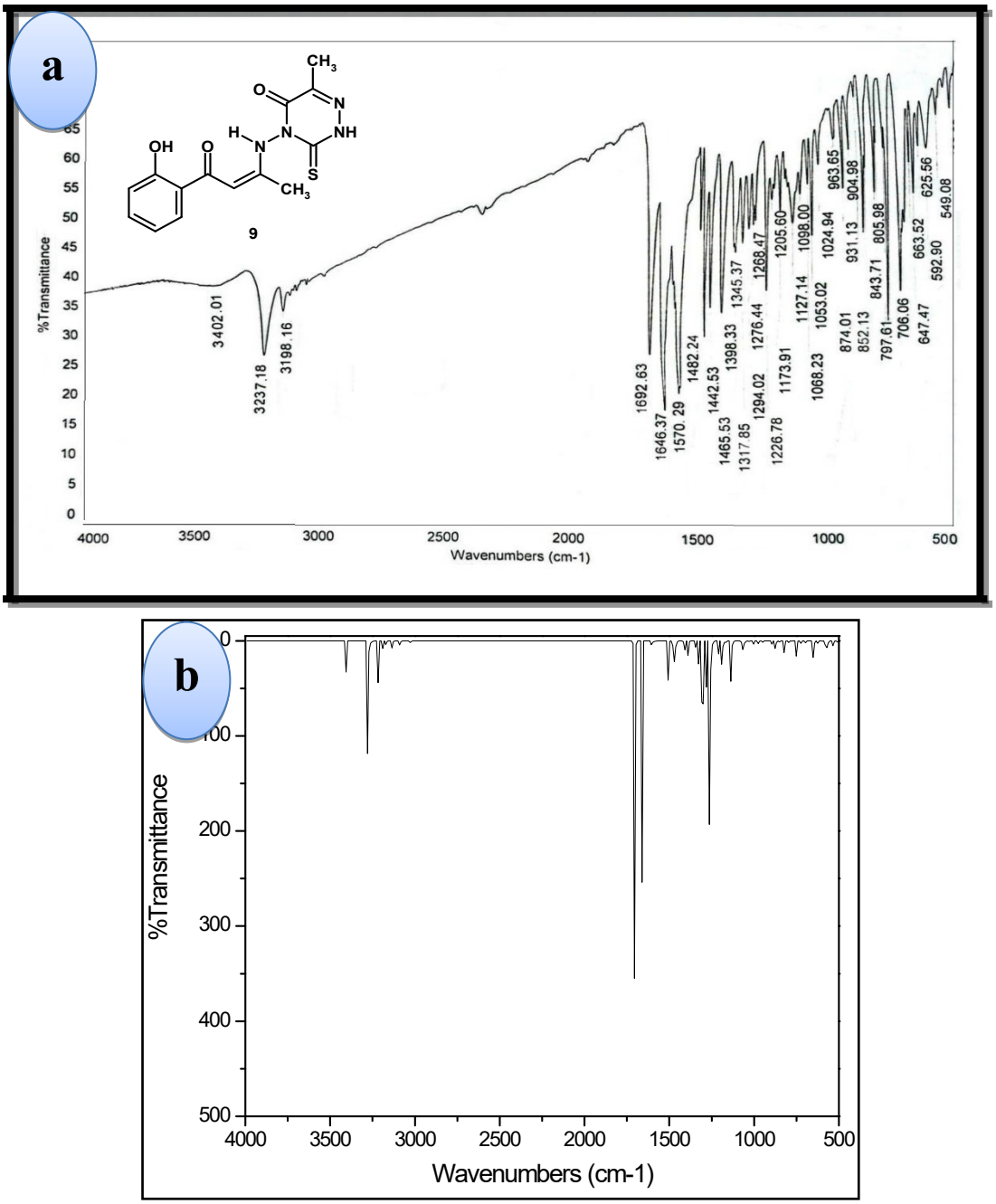

Fig. S22. (a) Experimental and (b) Calculated IR spectra of compound **9** at B3LYP/6-311++G(d,p).

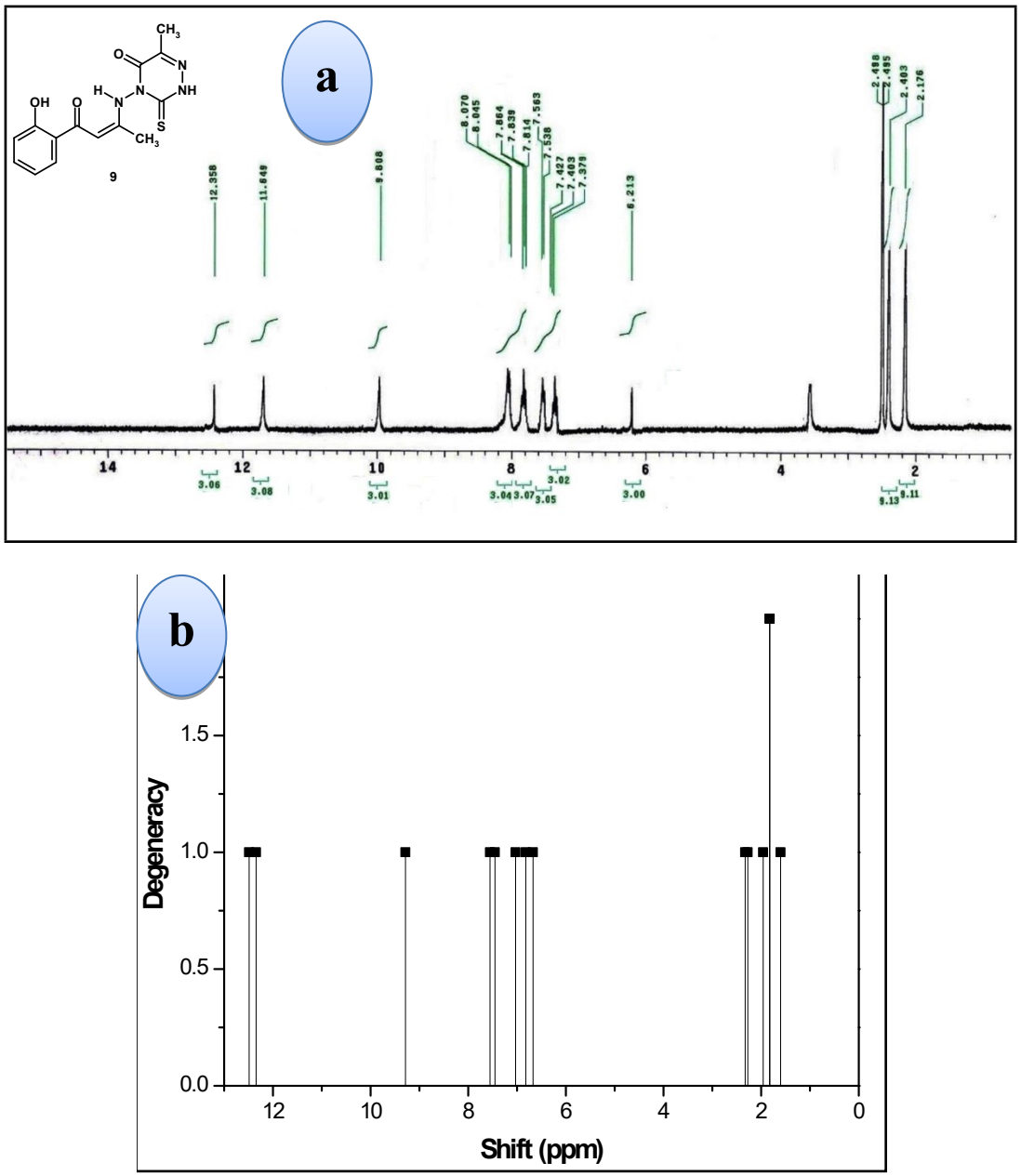

Fig. S23. (a) Experimental and (b) Calculated ^{1}H NMR spectra of compound **9** at B3LYP/6-311++G(d,p).

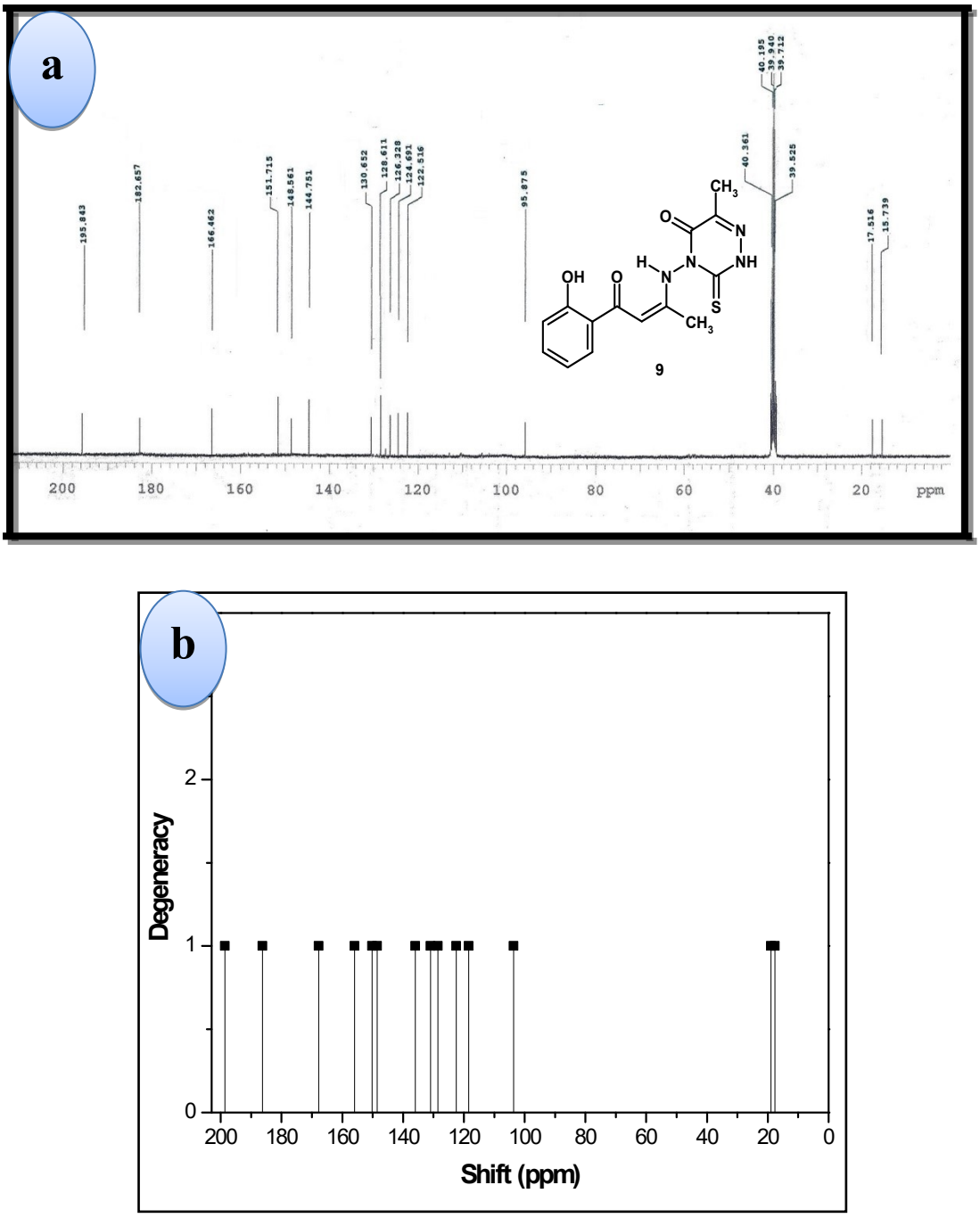

Fig. S24. (a) Experimental and (b) Calculated ^{13}C NMR spectra of compound **9** at B3LYP/6-311++G(d,p).

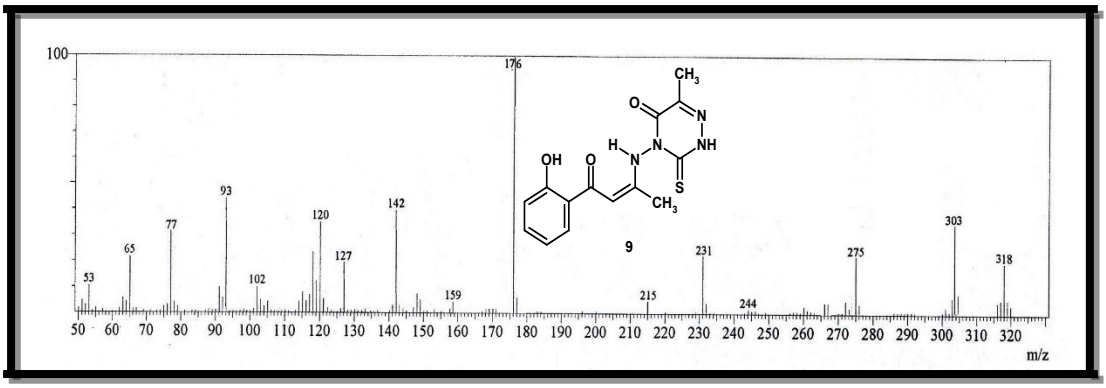

Fig. S25. Mass spectrum of compound **9**

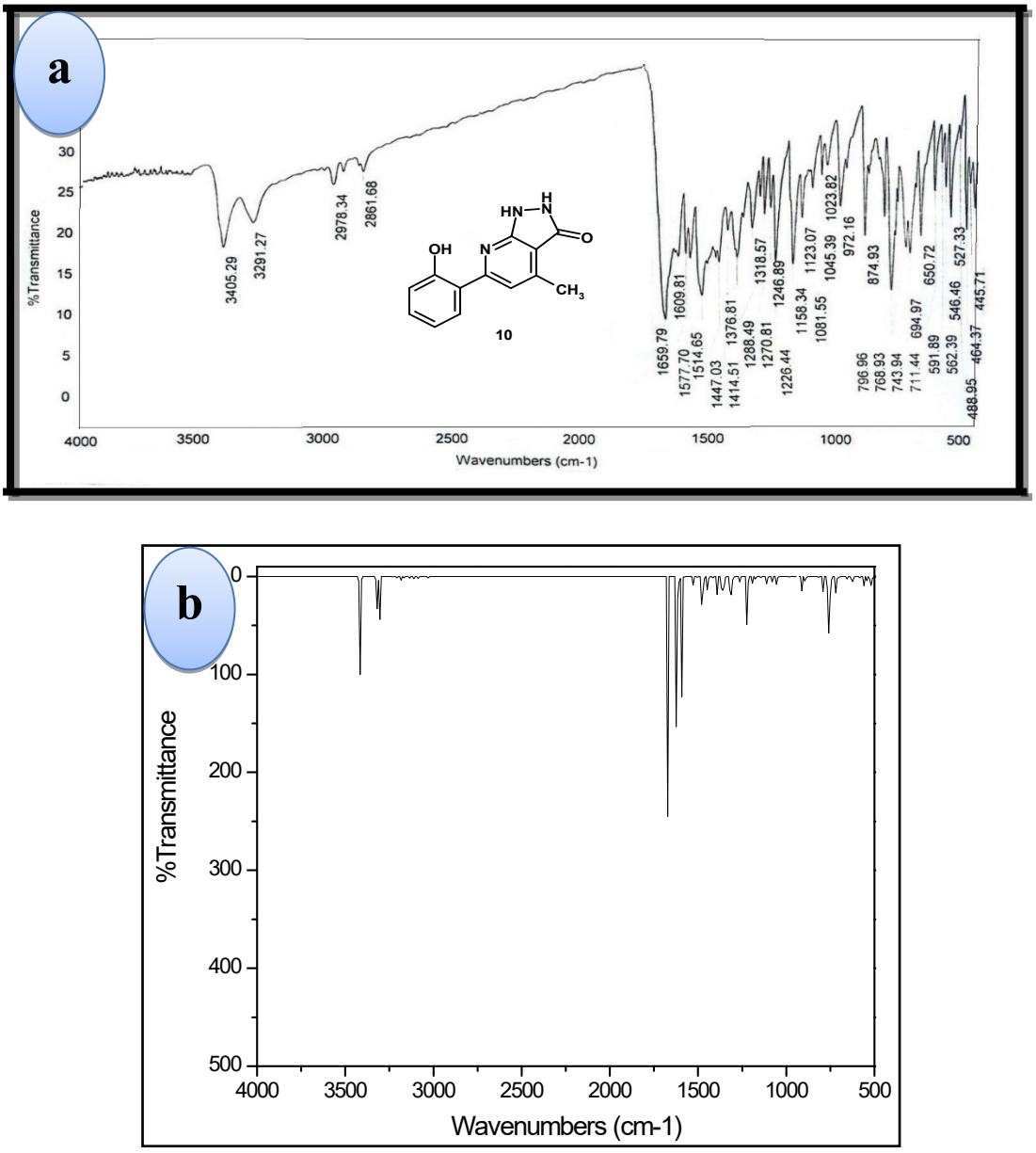

Fig. S26. (a) Experimental and (b) Calculated IR spectra of compound **10** at B3LYP/6-311++G(d,p).

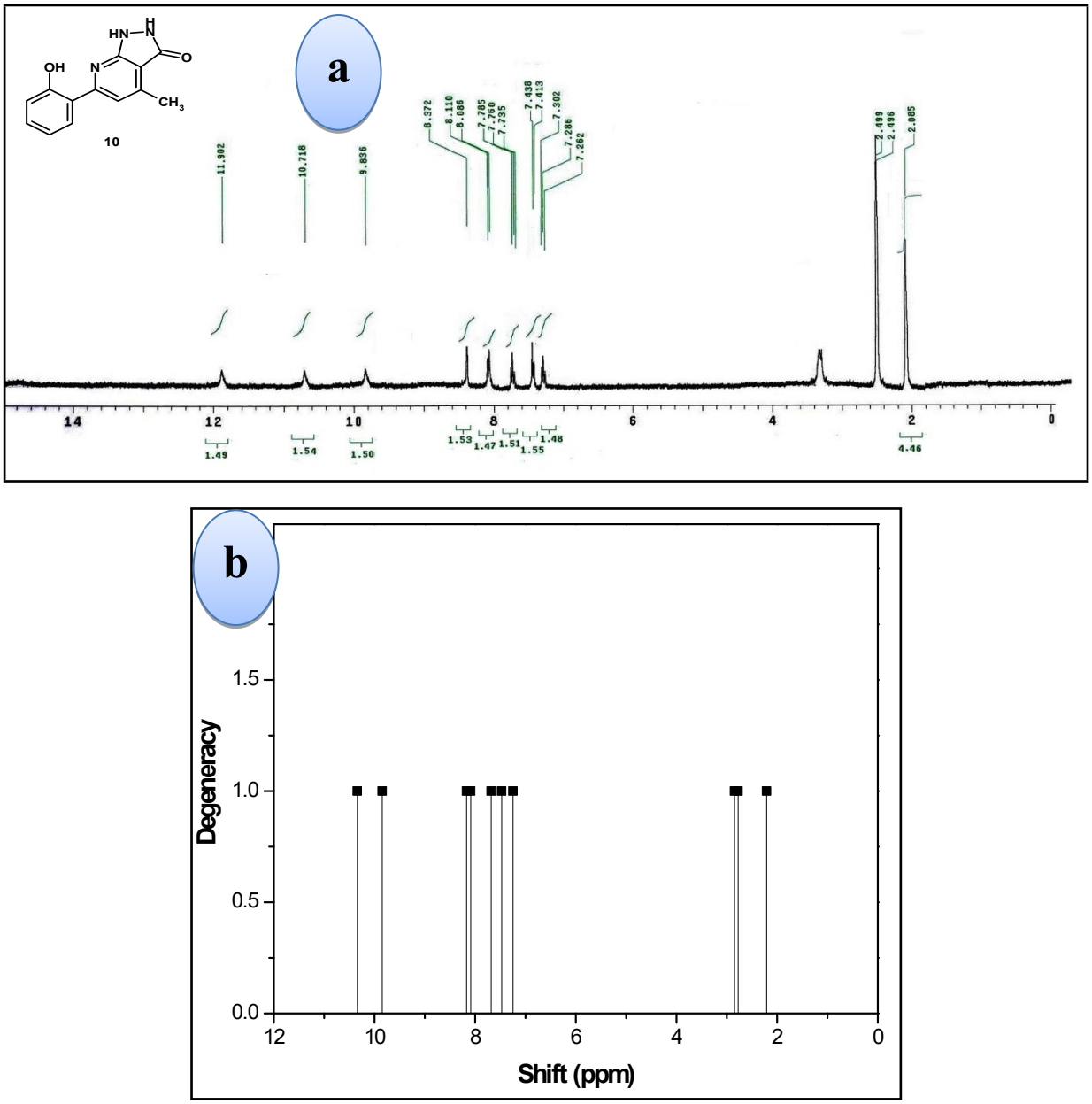

Fig. S27. (a) Experimental and (b) Calculated ^{1}H NMR spectra of compound **10** at B3LYP/6-311++G(d,p).

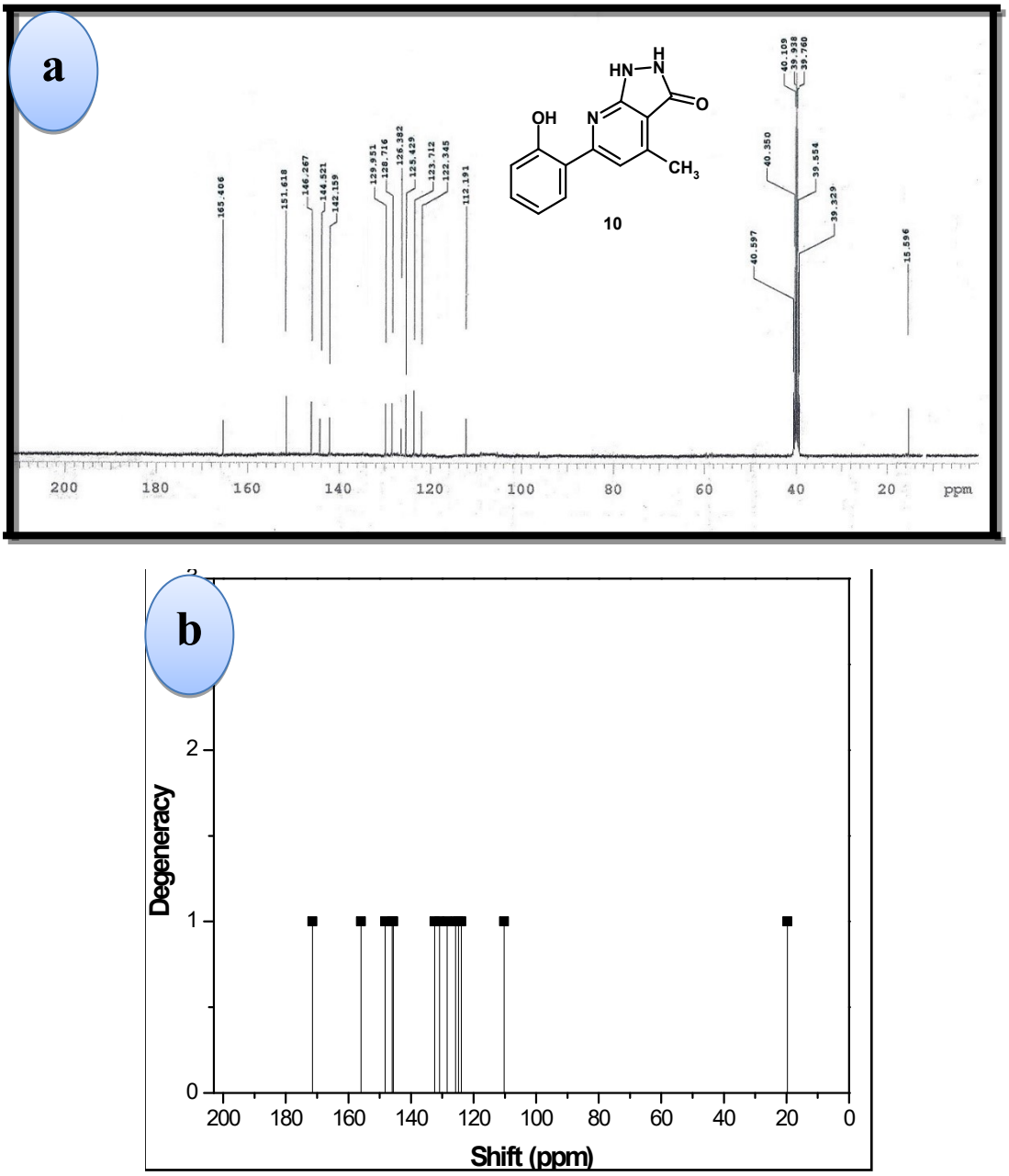

Fig. S28. Experimental and Calculated ^{13}C NMR spectra of compound **10** at B3LYP/6-311++G(d,p).

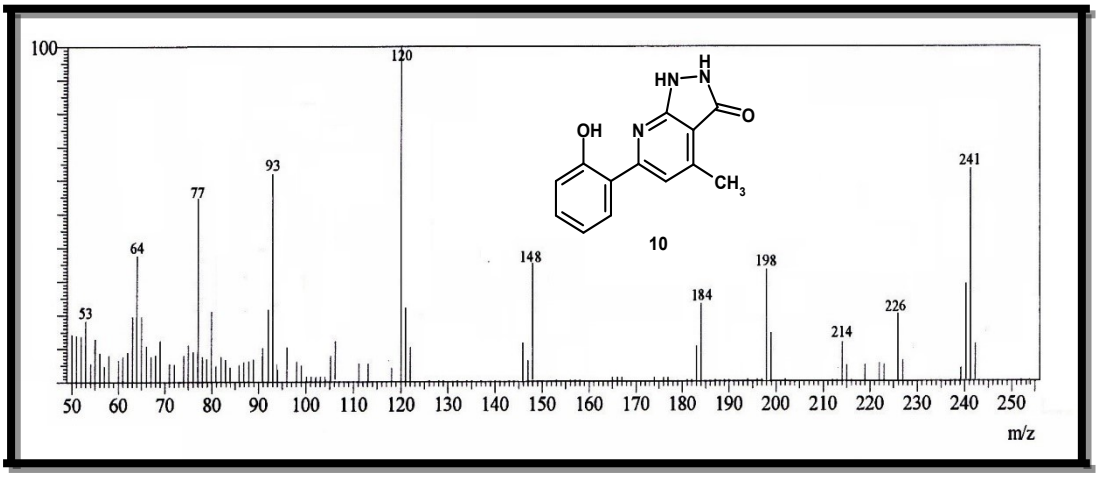

Fig. S29. Mass spectrum of compound **10**

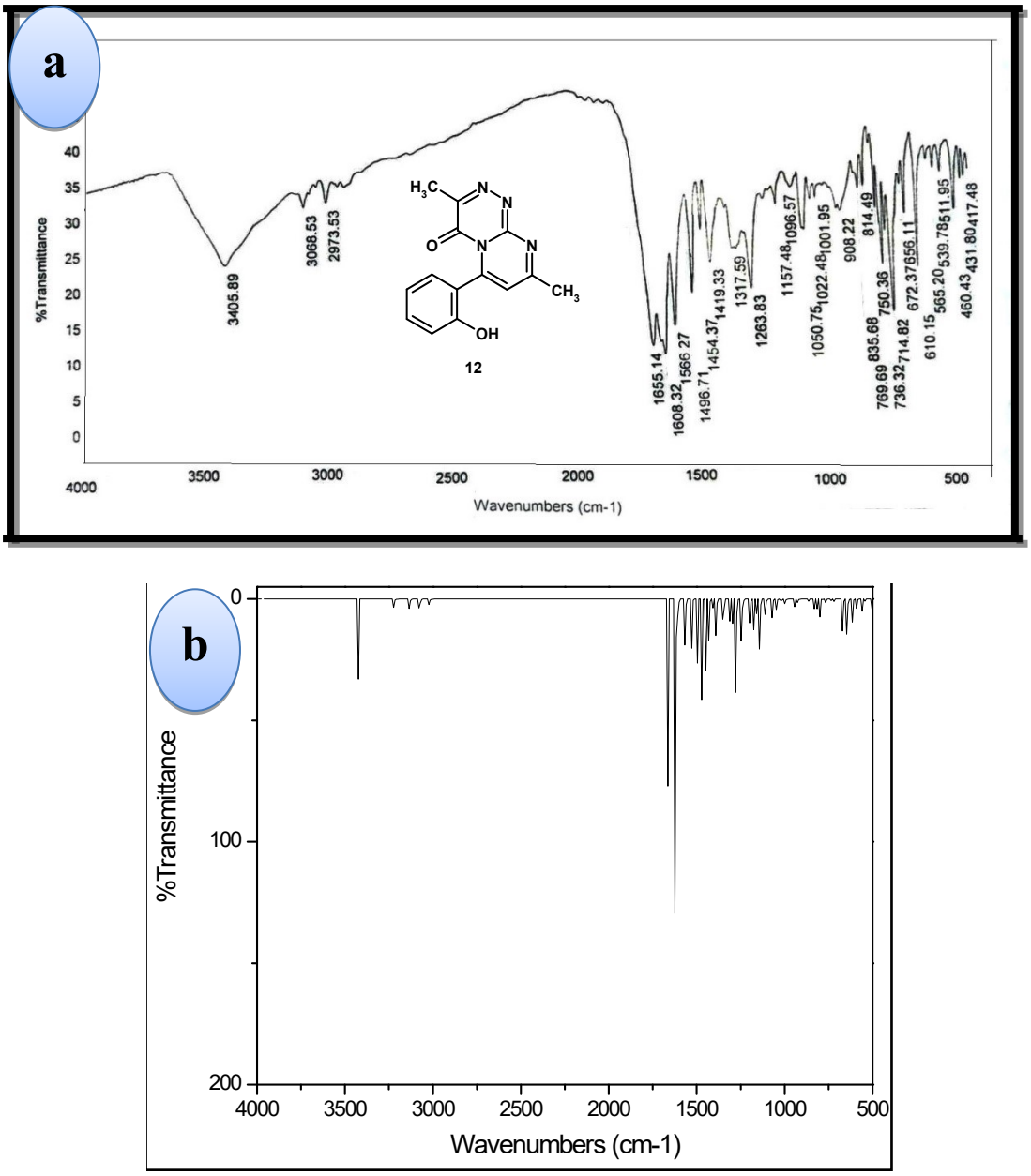

Fig. S30. (a) Experimental and (b) Calculated IR spectra of compound **12** at B3LYP/6-311++G(d,p).

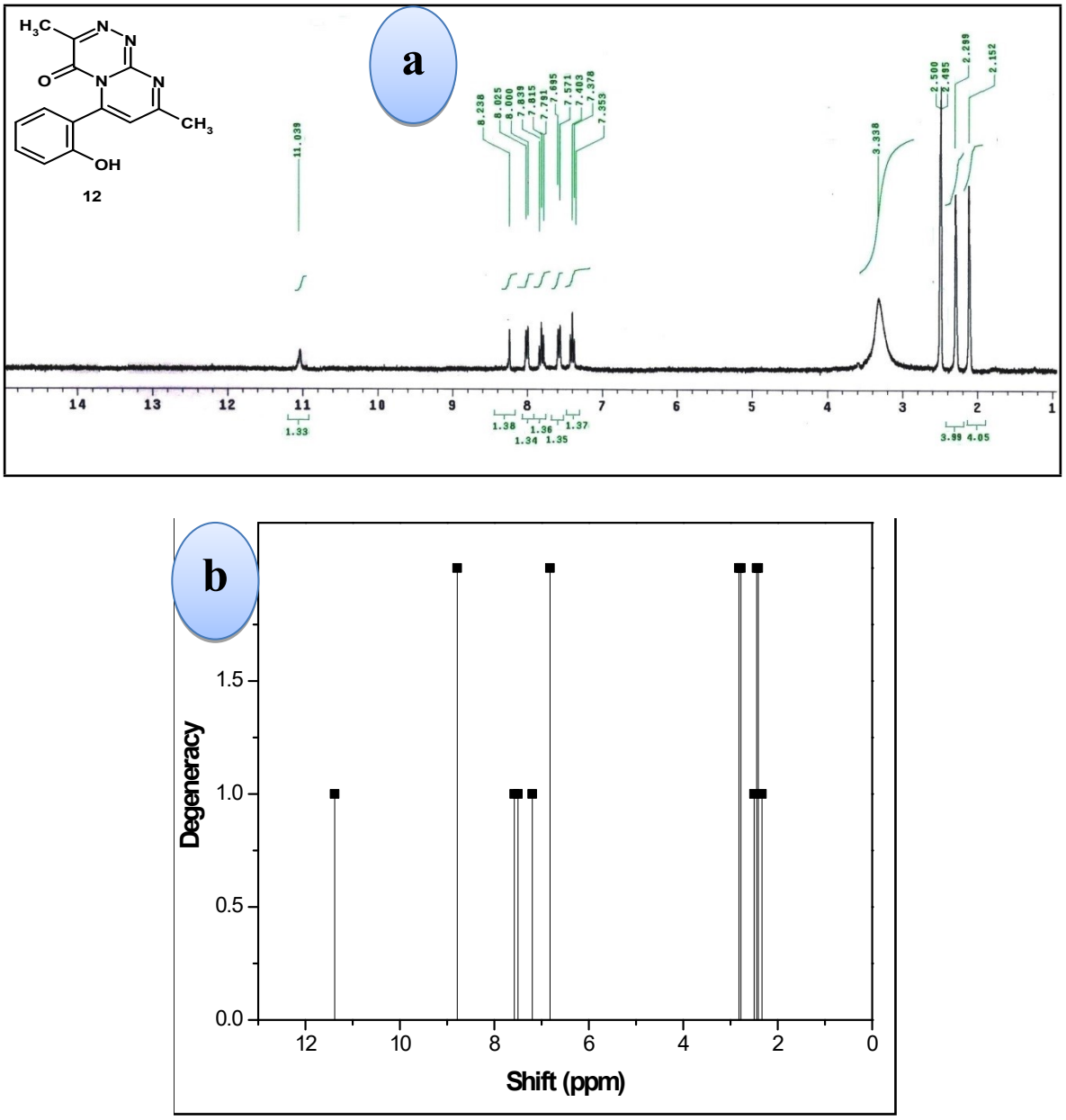

Fig. S31. (a) Experimental and (b) Calculated ^{1}H NMR spectra of compound **12** at B3LYP/6-311++G(d,p).

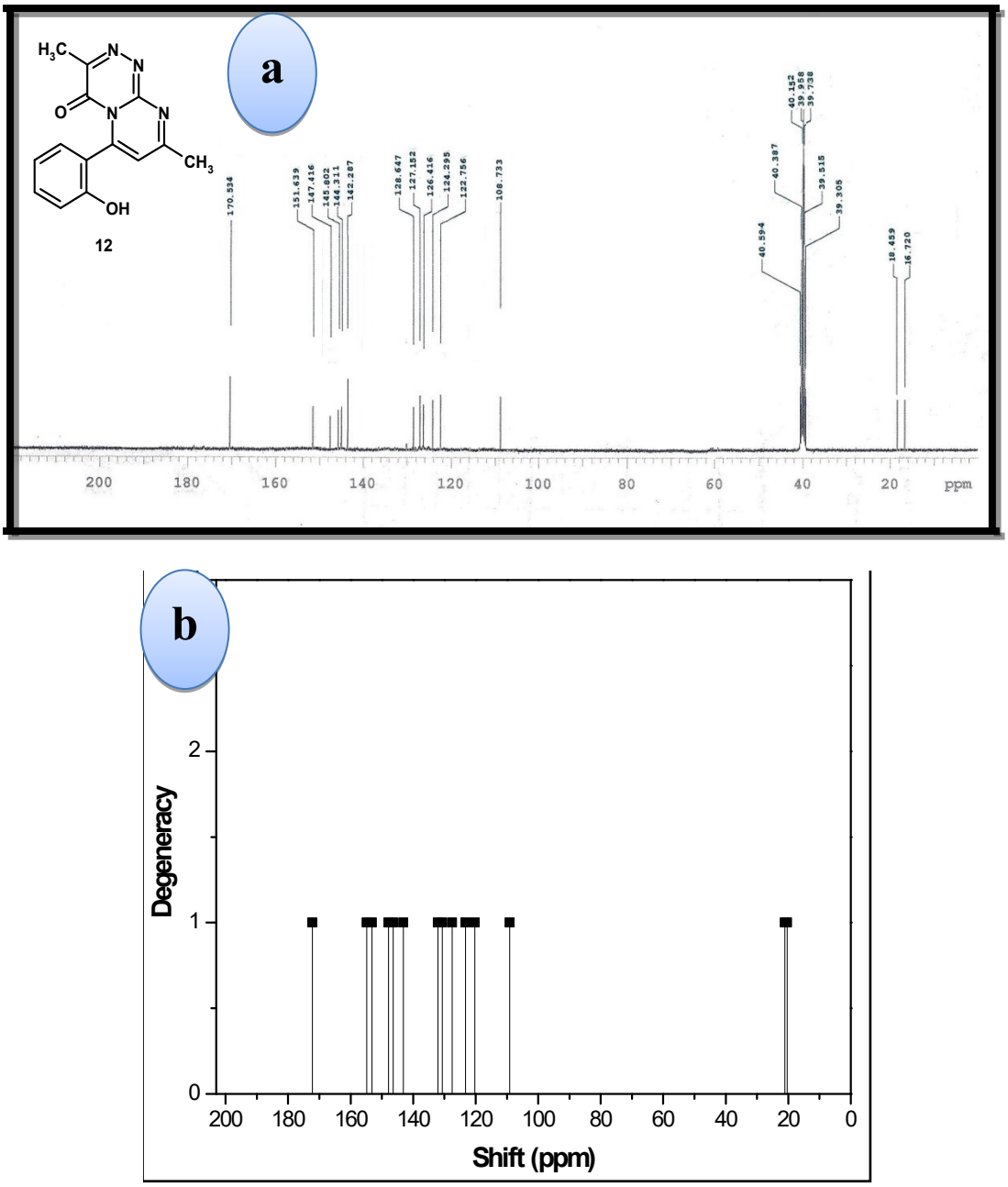

Fig. S32. Experimental and Calculated ^{13}C NMR spectra of compound **12** at B3LYP/6-311++G(d,p).

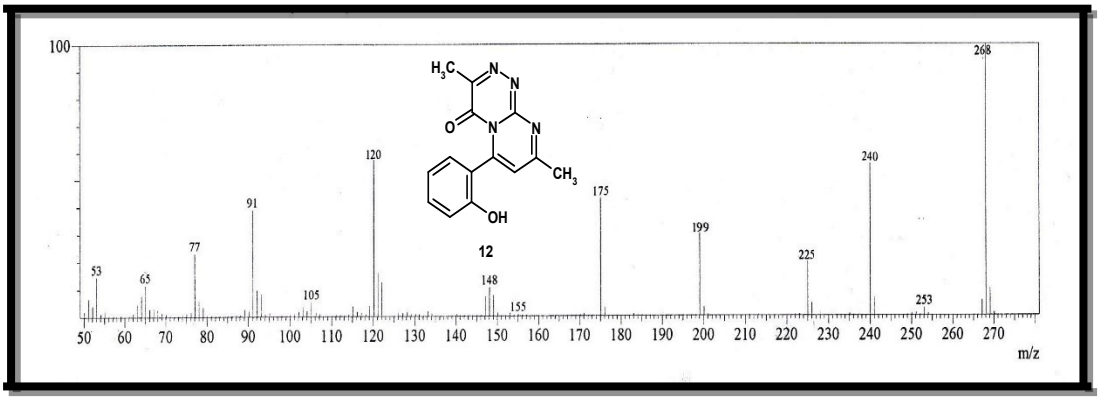

Fig. S33. Mass spectrum of compound **12**

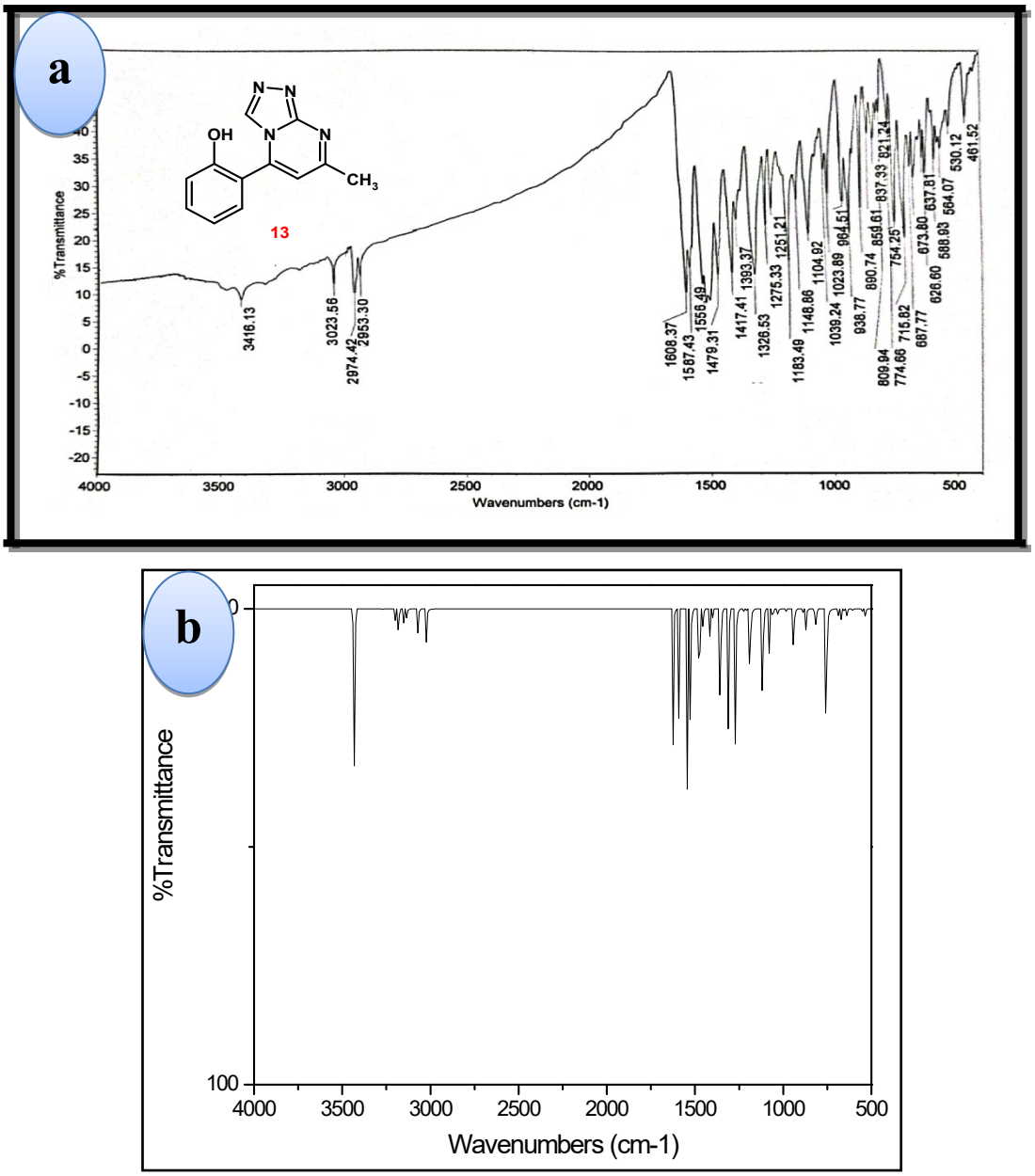

Fig. S34. (a) Experimental and (b) Calculated IR spectra of compound **13** at B3LYP/6-311++G(d,p).

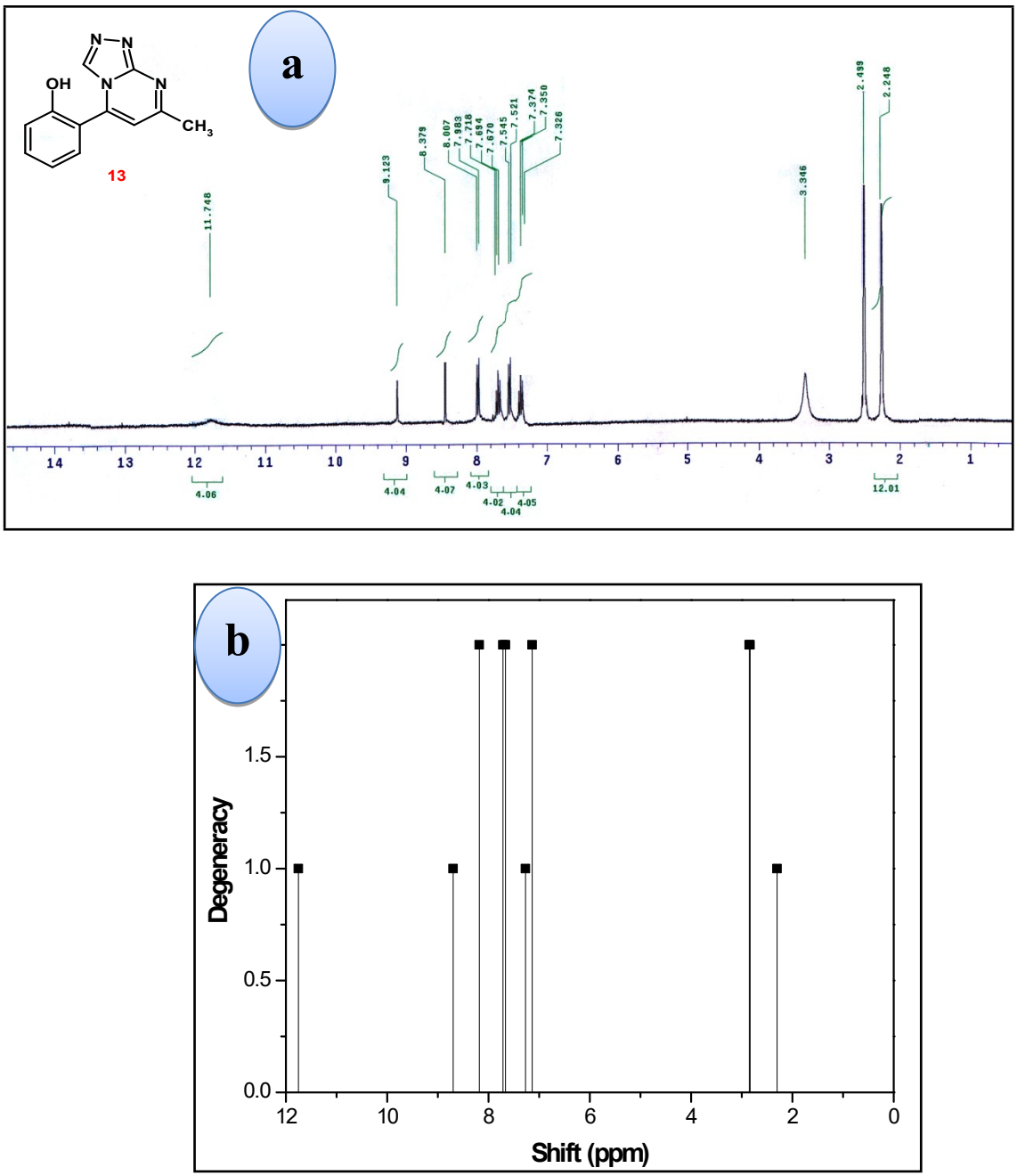

Fig. S35. (a) Experimental and (b) Calculated ^{1}H NMR spectra of compound **13** at B3LYP/6-311++G(d,p).

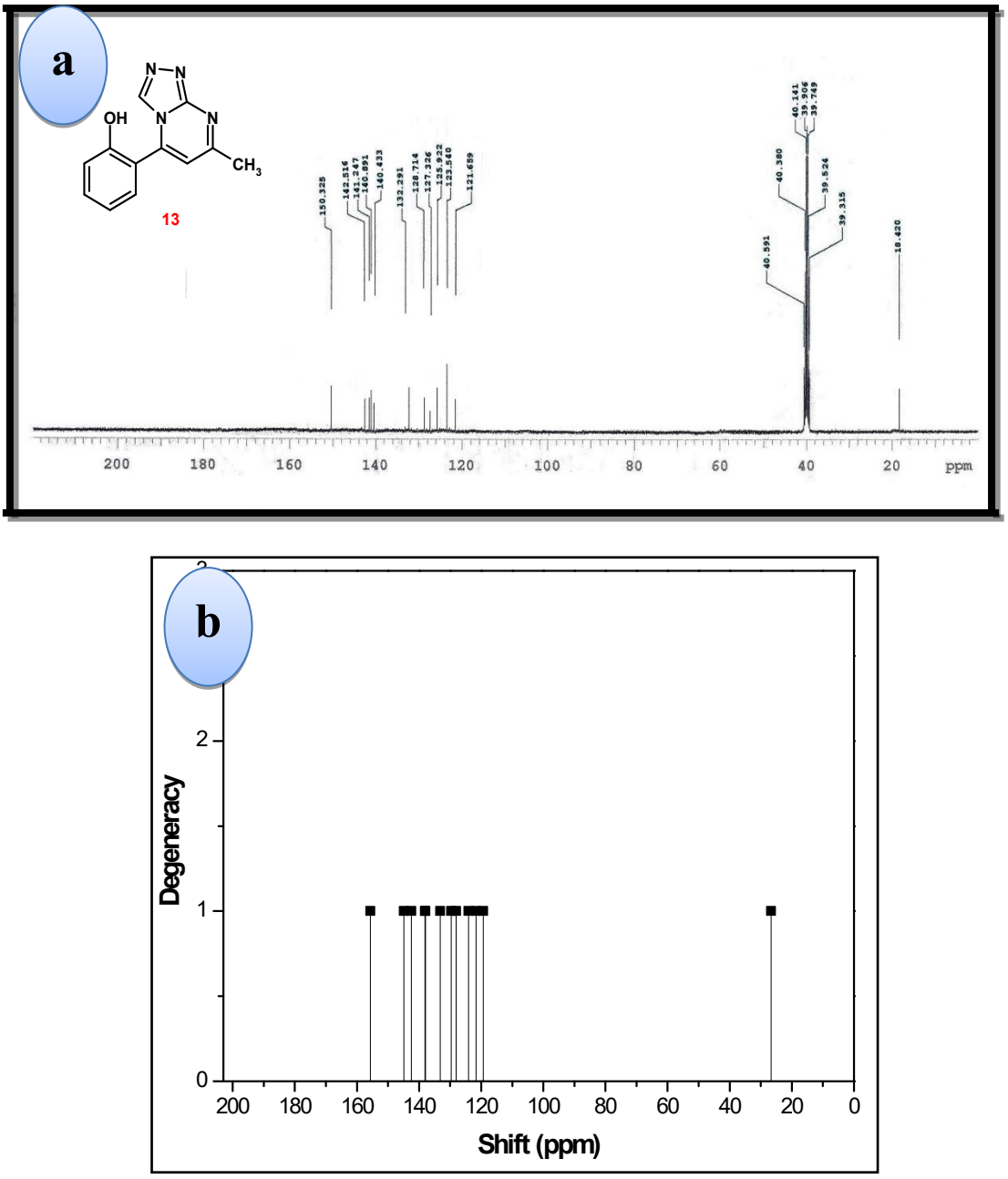

Fig. S36. Experimental and Calculated ^{13}C NMR spectra of compound **13** at B3LYP/6-311++G(d,p).

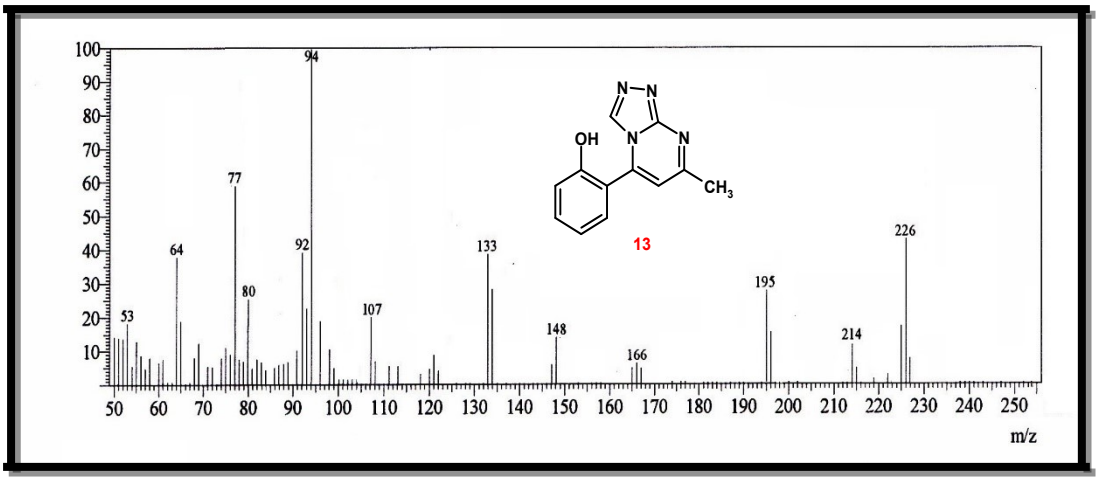

Fig. S37. Mass spectrum of compound **13**

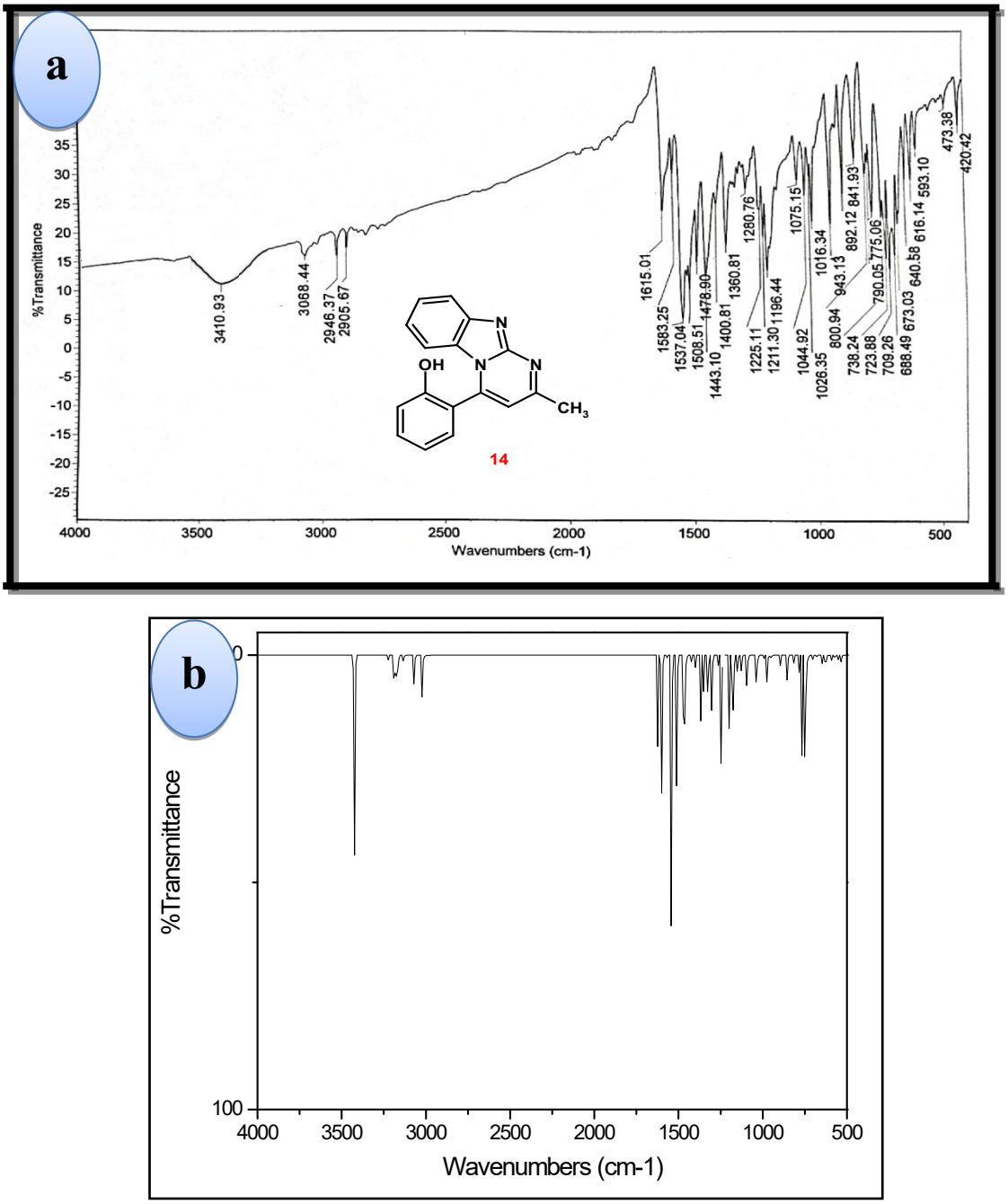

Fig. S38. (a) Experimental and (b) Calculated IR spectra of compound **14** at B3LYP/6-311++G(d,p).

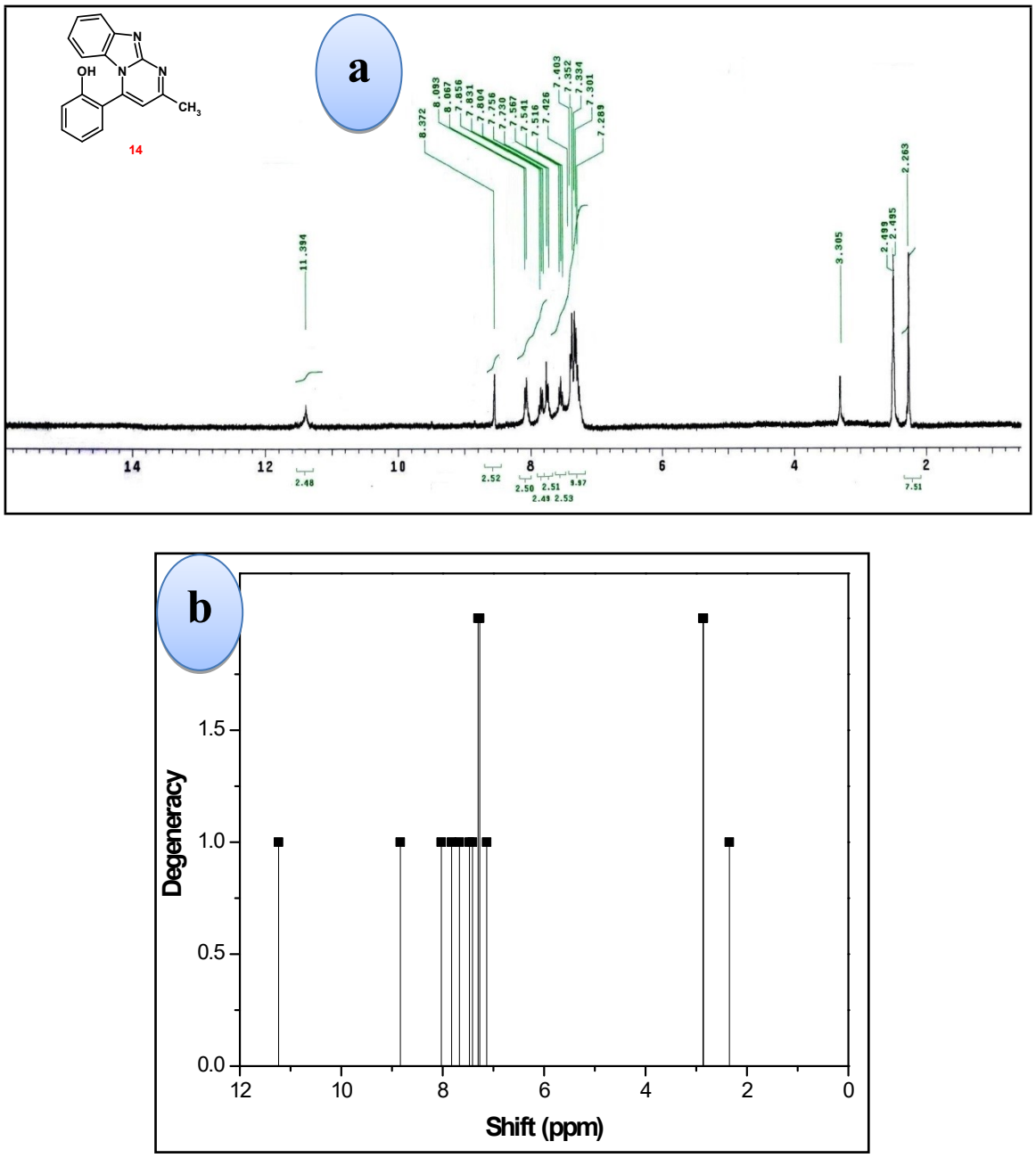

Fig. S39. Experimental and Calculated ^{1}H NMR spectra of compound **14** at B3LYP/6-311++G(d,p).

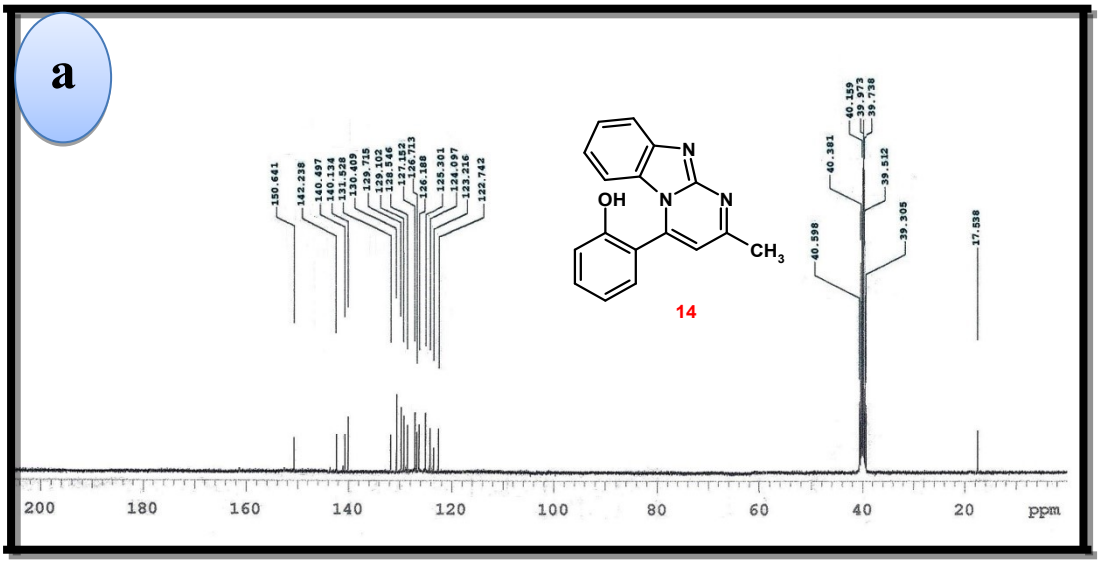

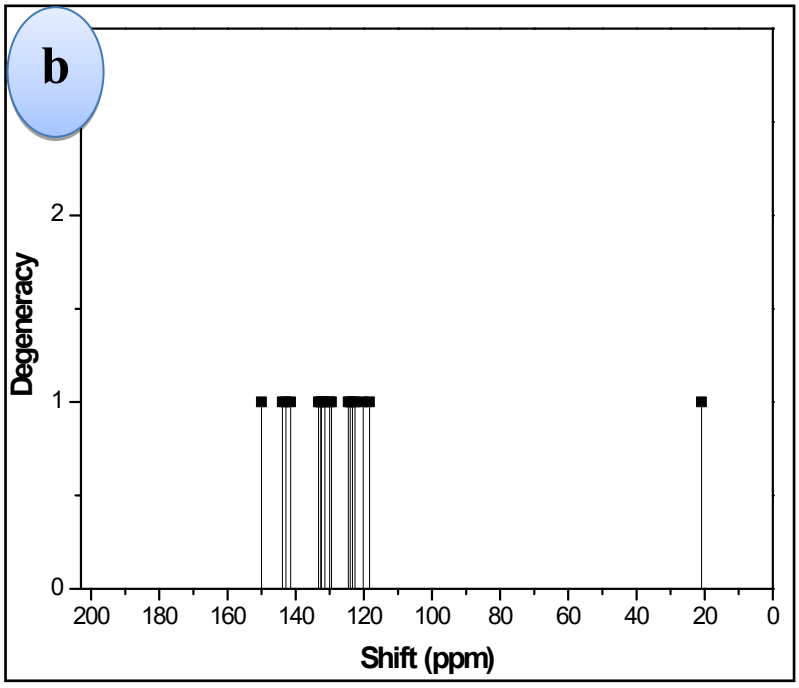

Fig. S40. Experimental and Calculated ^{13}C NMR spectra of compound **14** at B3LYP/6-311++G(d,p).

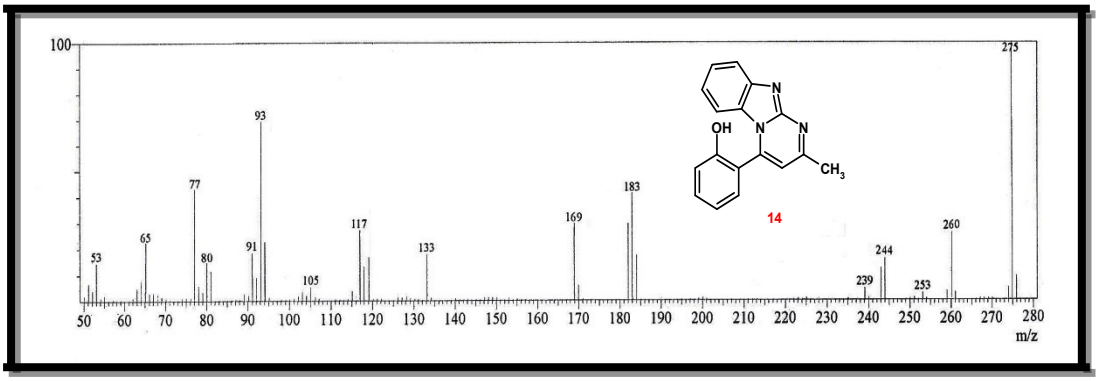

Fig. S41. Mass spectrum of compound **14**

Fig. S42. The bioavailability radars of compounds **9-10** and **12-14**

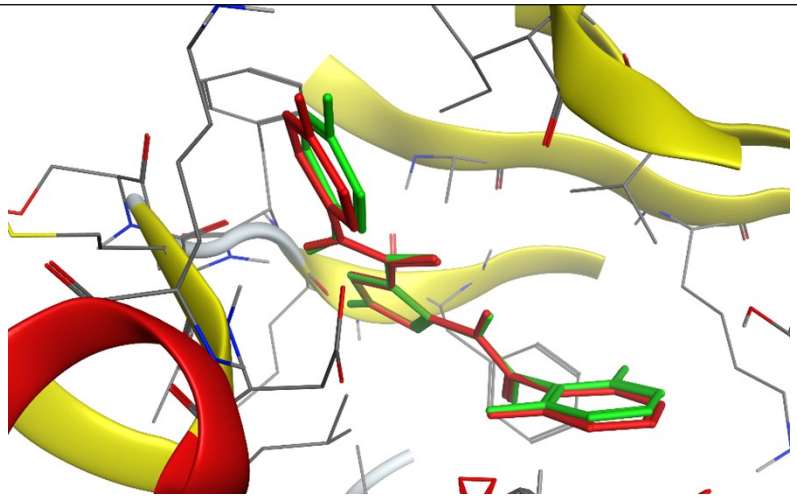

Fig. S43. 3D representation of the superimposition of the co-crystallized (red) and the redocking pose (green) of the ([(2,6-difluorophenyl)carbonyl]amino)-N-(4-fluorophenyl)-1H-pyrazole-3-carboxamide ligand in target protein (pdb ID: 4Y72).

Compound	3D	Compound	3D
1	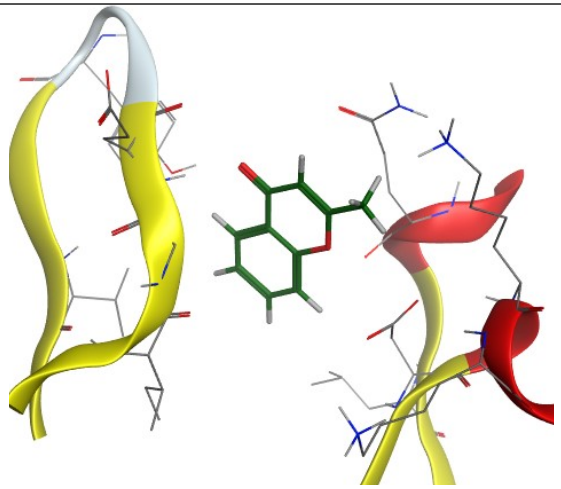	**10**	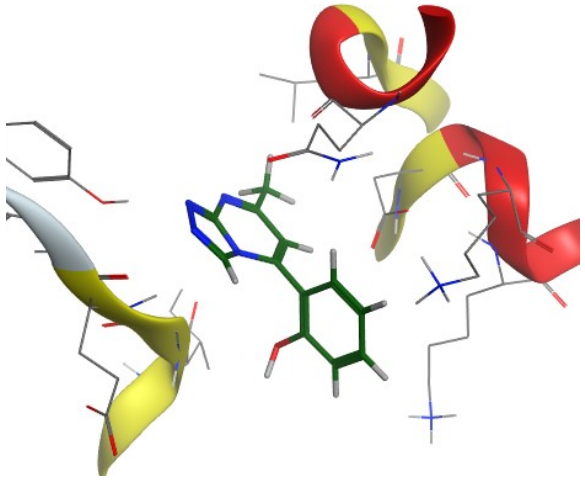
12	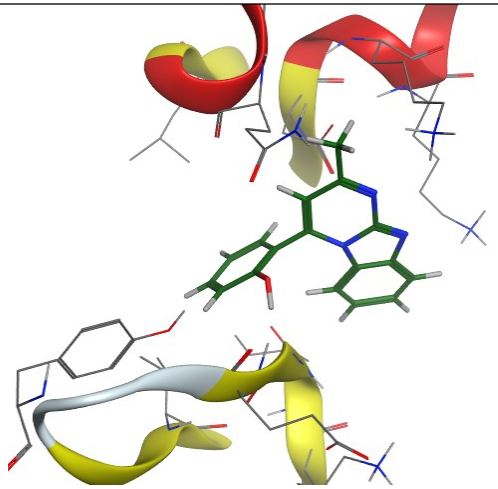	**13**	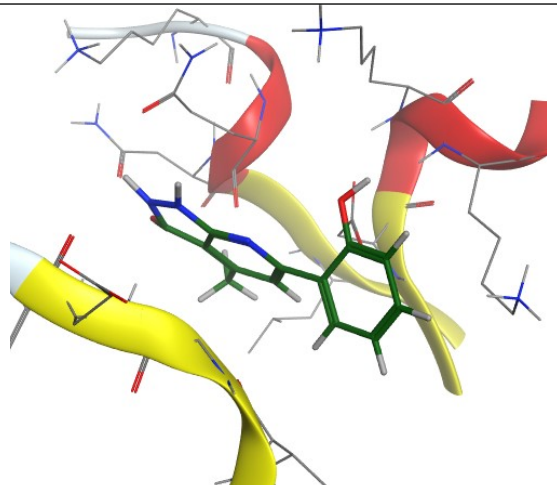

Fig. S44. 3D representation of the hydrogen bonding between the studied compounds (**1**, **10**, **12** and **13**) with the amino acids residues of the target protein (PDB ID: 4Y72).

Table S1. Various interactions between the studied compounds **1**, **10**, **12** and **13** with the amino acids residues of the target protein (pdb ID: 4Y72).

Compound 1 (Binding energy -7.6 kcal/mol)			**Compound 10** (Binding energy -7.80 kcal/mol)		
Receptor	Distance	Interaction Type	Receptor	Distance	Interaction Type
GLU12	2.07	H-Bond	GLU12	2.94	H-Bond
LYS88	4.31	Alkyl	ASP86	4.60	Pi-Anion
			GLU12	2.70	Pi-Donor
Compound 12 (Binding energy -7.60 kcal/mol)			**Compound 13** (Binding energy -8.10 kcal/mol)		
ASP86	3.45	Pi-Anion	GLN132	2.20	H-Bond
ASP86	3.71	Pi-Anion	ASP86	4.21	Pi-Anion
ASP86	4.43	Pi-Anion	ASP86	4.93	Pi-Anion
GLY11	3.83	Pi-Sigma	LYS89	4.98	Pi-Alkyl
ILE10	2.82	Pi-Lone Pair			
LYS88	5.34	Pi-Alkyl			
LYS89	5.38	Pi-Alkyl			
VAL18	5.10	Pi-Alkyl			
Co-crystallized ligand (Binding energy -10.60 kcal/mol)					
LEU83	2.1229	H-Bond			
GLU81	1.66193	H-Bond			
ASP146	4.75511	Pi-Anion			
VAL18	3.99529	Pi-Sigma			
LEU135	3.50724	Pi-Sigma			
ILE10	4.07235	Pi-Alkyl			
ALA31	3.38275	Pi-Alkyl			
VAL64	5.26978	Pi-Alkyl			
LEU83	5.45921	Pi-Alkyl			
ALA145	5.06422	Pi-Alkyl			